J. Membrane Biol. 93, 111–132 (1986)

The Journal of
Membrane Biology

Voltage-Dependent Channel Formation by Rods of Helical Polypeptides

Gianfranco Menestrina†*, Klaus-Peter Voges‡, Günther Jung‡, and Günther Boheim†
†Department Zellphysiologie, Ruhr-Universität Bochum, D-4630 Bochum, Federal Republic of Germany, and
‡Institut für Organische Chemie, Universität Tübingen, D-7400 Tübingen, Federal Republic of Germany

Summary. The voltage-dependence of channel formation by alamethicin and its natural analogues can be described by a dipole flip-flop gating model, based on electric field-induced transbilayer orientational movements of single molecules. These field-induced changes in orientation result from the large permanent dipole moment of alamethicin, which adopts α-helical conformation in hydrophobic medium. It was, therefore, supposed that the only structural requirement for voltage-dependent formation of alamethicin-type channels might be a rigid lipophilic helical segment of minimum length.

In order to test this hypothesis we synthesized a family of lipophilic polypeptides—Boc-(Ala-Aib-Ala-Aib-Ala)$_n$-OMe, n = 1–4 — which adopt α-helical conformation for n = 2 – 4 and studied their interaction with planar lipid bilayers. Surprisingly, despite their large difference in chain length, all four polypeptides showed quanlitatively similar behavior. At low field strength of the membrane electric field these polypeptides induce a significant, almost voltage-independent increase of the bilayer conductivity. At high field strength, however, a strongly voltage-dependent conductance increase occurs similar to that observed with alamethicin. It results from the opening of a multitude of ion translocating channels within the membrane phase.

The steady-state voltage-dependent conductance depends on the 8th–9th power of polypeptide concentration and involves the transfer of 4–5 formal elementary charges. From the power dependences on polypeptide concentration and applied voltage of the time constants in voltage-jump current-relaxation experiments, it is concluded that channels could be formed from preexisting dodecamer aggregates by the simultaneous reorientation of six formal elementary charges. Channels exhibit large conductance values of several nS, which become larger towards shorter polypeptide chain length. A mean channel diameter of 19 Å is estimated corresponding roughly to the lumen diameter of a barrel comprised of 10 α-helical staves. Similar to experiments with the N-terminal Boc-derivative of alamethicin we did not observe the burst sequence of nonintegral conductance steps typical of natural (N-terminal Ac-Aib)-alamethicin. Saturation in current/voltage curves as well as current inactivation in voltage-jump current-relaxation experiments are found. This may be understood by assuming that channels are generated as dodecamers but, while reaching the steady state, reduce their size to that of an octamer or nonamer. We conclude that the overall behavior of these synthetic polypeptides is very similar to that of alamethicin. They exhibit the same concentration and voltage-dependences but lack the stabilizing principle of resolved channel states characteristic of alamethicin.

Key Words planar lipid bilayers · alamethicin · α-helix dipole · dipole moment · voltage-dependent gating · flip-flop mechanism

Introduction

The eicosapeptide alamethicin as well as its natural peptaibol analogues suzukacillin and trichotoxin form voltage-dependent ion translocating pathways in lipid bilayer membranes (Mueller & Rudin, 1968; Gordon & Haydon, 1972; Eisenberg, Hall & Mead, 1973; Boheim, 1974; Boheim et al., 1976; Hanke et al., 1983). These peptides have many structural features in common. They comprise a large number of the α,α-dimethylated amino acid Aib in their sequence (Brückner & Przybylski, 1984; Brückner et al., 1985; Katz et al., 1985; Schmitt & Jung, 1985*a*,*b*). The N-terminal part consists mainly of lipophilic amino acids, whereas the C-terminus is more hydrophilic. A proline is found in position 14 (or 13 in trichotoxin), and finally they adopt α-helical conformation. The respective helix elongates on transference from aqueous to lipophilic environment (Jung, Dubischar & Leibfritz, 1975; Butters et al., 1981; Fox & Richards, 1982; Bosch et al., 1984).

The voltage dependence of channel formation as well as the typical sequence of discrete nonintegral conductance levels in a single fluctuating alamethicin channel have been explained by Boheim, Hanke and Jung (1983) on the basis of a dipole flip-flop gating mechanism. In this model the membrane electric field is sensed by the permanent dipole moment of the α-helical part of the molecule, which spans the hydrophobic bilayer core. Alamethicin molecules in antiparallel orientation aggregate within the membrane plane in the absence of an

* *Present address:* Dipartimento di Fisica, Universita di Trento, I-38050 Povo, Italy.

Table 1. Amino acid sequences of natural and synthetic polypeptides studied

Alamethicin F30—main component (Schmitt & Jung, 1985*a,b*)
Ac-Aib-Pro-Aib-Ala-Aib-Ala-Gln-Aib-Val-Aib-Gly-Leu-Aib- 1 5 10 Pro-Val-Aib-Aib-Glu-Gln-Pheol 15 20
Antiamoebin (Rinehart et al., 1977; Brückner et al., 1980)
Ac-Phe-Aib-Aib-Aib-Iva-Gly-Leu-Aib-Aib-Hyp-Gln-Iva-Hyp-Aib-Pro-Pheol
Trichotoxin fragment—TT 13-18 (Brückner & Jung, 1982)
H-Pro-Leu-Aib-Aib-Gln-Valol
Synthetic peptides—P20, P15, P10 and P5 (Voges, 1985)
Boc-(Ala-Aib-Ala-Aib-Ala)$_n$-OMe
with n = 4 (P20), n = 3 (P15), n = 2 (P10), n = 1 (P5)
Synthetic peptide—P11 (Bosch et al., 1985*a*)
Boc-Ala-Aib-Ala-Aib-Ala-Glu(OBzl)-Ala-Aib-Ala-Aib-Ala-OMe
Synthetic peptide—P9 (Bosch et al., 1985*b*)
Boc-Leu-Aib-Pro-Val-Aib-Aib-Glu(OBzl)-Gln-Pheol
Synthetic peptide—P5a (Bosch, Jung & Winter, 1983)
Boc-Aib-Ala-Aib-Ala-Aib-OMe
Synthetic peptide—Poly(AAG) (ref. Drs. Brack and Spach, Orleans)
HCO-(L-Ala-L-Ala-Gly)$_m$-OMe, mixture of various m values

Abbreviations: Ac, acetyl; Aib, α-aminoisobutyric acid; Boc, *t*-butyloxycarbonyl; Bzl, benzyl; Iva, D-isovaline; Hyp, hydroxyproline; Me, methyl; Pheol, L-phenylalaninol; Valol, L-valinol. Except of Iva all other chiral amino acids have L-configuration.

electric field. Upon application of a sufficiently large voltage these aggregates are converted into arrays of parallel helices, which form water-filled ion conducting channels. Large dipole moments of 60–75 D have been determined for alamethicin (Schwarz & Savko, 1982; Yantorno, Takashima & Mueller, 1982) and trichotoxin A40 (Schwarz, Savko & Jung, 1983). Elementary dipoles originate from the charge separation phenomenon at peptide bonds (Hol et al., 1978) and sum up to macrodipoles in case of rods of helical structure (Hol, Halie & Sander, 1981; Hol, 1985). This general concept of α-helical dipoles was confirmed by X-ray structure analysis (Butters et al., 1981) and dipole moment measurements (Rizzo, Schwarz, Voges & Jung, 1985) of synthetic α-helical polypeptides. The same polypeptides as used by these authors were also tested in our studies.

Two observations indicate that voltage-dependent channel formation by alamethicin-type polypeptides results from its intrinsic dipole moment, whereas resolved single channel current records seem to require additionally the presence of particular end groups and possibly a minimum length of the α-helix. First, the N-terminal Boc-derivative of highly pure synthetic alamethicin induces noisy events of large current amplitudes, while the strongly nonlinear current/voltage characteristic remains virtually unchanged (Jung et al., 1983a; S. Gelfert-Peukert and G. Boheim, *in preparation*). Second, the natural analogue trichotoxin A40 is different from alamethicin (it is missing one amino acid near the N-terminal end and has only one glutamine at the C-terminal end), but the typical voltage-dependent conductance increase can be observed, even though stable channel-state current levels could not be resolved (Hanke *et al.*, 1983). The structural feature in common with all the polypeptide antibiotics considered seems to be the presence of an α-helix, consistent with the dipole flip-flop gating model. It is the α-helical dipole which causes the expression of the voltage-dependent conductance increase in lipid bilayer membranes.

In order to elucidate the minimum conformational requirements for the formation of voltage-dependent alamethicin-type channels, we synthesized a series of Aib-containing peptides: Boc-(L-Ala-Aib-Ala-Aib-Ala)$_n$-OMe (n = 1 − 4), abbreviated in the following as polypeptides P5, P10, P15 and P20. Each of the four polypeptides forms voltage-dependent channels of large size, which are described in their concentration and voltage-dependence by the same analytical expressions as used with alamethicin. The flip-flop gating mechanism turns out to be the best framework for an understanding of the molecular mechanisms which lead to voltage-dependent formation of this type of channels. A preliminary report on part of the data has previously been presented (Jung et al., 1983*b*).

For observing these channels, membrane voltages larger than 150 mV had to be applied. For comparison we also studied at these high voltages the behavior of alamethicin and antiamoebin, a natural Aib-containing hexadecapeptide antibiotic (Rinehart et al., 1977; Brückner et al., 1980), which is remotely related to alamethicin.

Materials and Methods

Polypeptides

Polypeptides investigated in our experiments are listed in Table 1 with their complete sequence and corresponding references for the chemical work. Natural polypeptides were alamethicin F30, antiamoebin and the hexapeptide fragment from the C-terminus of trichotoxin (TT 13–18). Synthetic polypeptides were Boc-(Ala-Aib-Ala-Aib-Ala)$_n$-OMe with n = 4 (P20), n = 3 (P15), n = 2

(P10) and $n = 1$ (P5), respectively. In addition, we tested the peptides Boc-Ala-Aib-Ala-Aib-Ala-Glu(OBzl)-Ala-Aib-Ala-Aib-Ala-OMe (P11), Boc-Leu-Aib-Pro-Val-Aib-Aib-Glu(OBzl)-Gln-Pheol (P9) which is identical to the C-terminal nonapeptide of alamethicin and Boc-Aib-Ala-Aib-Ala-Aib-OMe (P5a). The latter three polypeptides have been crystallized and helical structure was determined by X-ray crystallography (Jung et al., 1983*b*; Bosch, Jung, Schmitt & Winter, 1985*a*). All these polypeptides were added to the bilayer bathing electrolyte from ethanolic stock solutions. An additional series of experiments was carried out with synthetic HCO-(Ala-Ala-Gly)$_m$-OMe which was a polypeptide mixture of various m values (Poly-AAG). This sample was kindly provided by Drs. G. Spach and A. Brack, Orleans. The synthetic HCO-(L-Ala-L-Ala-Gly)$_5$ was supposed to adopt β-helix structure, and ion channel formation similar to gramicidin A was reported (Urry, Bradley & Ohnishi, 1978). Poly-AAG was dissolved in trifluoroethanol/trifluoroacetic acid (95 : 5; vol/vol). In control experiments it was found that the electrical properties of planar bilayers were changed neither by ethanol, nor by trifluoroethanol in concentrations exceeding those used in our polypeptide experiments.

Bilayer Experiments

Virtually solvent-free planar lipid bilayer membranes were prepared at room temperature by the apposition of two monolayers following the technique of Montal and Mueller (1972). Lipid used was 1-oleoyl-2-palmitoyl-glycero-3-phosphocholine (1,2-OPPC) purchased from Avanti (Birmingham, AL) with a main phase transition temperature of $T_c = -9$°C (Davis et al., 1981). Results were similar using other synthetic lecithins. Monolayers were spread from a 5-mg/ml solution of 1,2-OPPC in hexane/ethanol (99 : 1). After solvent evaporation, membranes were formed on a hole in a hexadecane pretreated Teflon sandwich septum separating two aqueous compartment solutions of 4 ml volume. Typical membrane area was $1 - 2 \times 10^{-4}$ cm^2; larger areas have been avoided in order to prevent membrane electrical breakdown at large applied voltages. The electrolyte solution, if not otherwise specified, was 1 M KCl unbuffered. All solvents and salts were of p.A.-grade purity.

In a typical experiment: a membrane was formed and a square wave of ±50 mV amplitude and 1 Hz frequency applied for about one hour. Then the bilayer was tested at high voltages ($V_{max} = 300$ mV). If the bare membrane current remained unchanged, the desired amount of polypeptide was added symmetrically to both compartments. The ±50-mV square wave was applied for one additional hour. Thereafter measurements were carried out. For low temperature experiments bath temperature was lowered to 5–10°C by means of an external thermostat after completion of the above described procedure. The principle of the mechanical set-up and the electronic equipment has been described elsewhere (Boheim & Kolb, 1978). The compartment connected to virtual ground is called *trans* side. Hence positive voltages mean *cis* side compartment to be positive with respect to the *trans* side. Positive currents are those for cations flowing from *cis* to *trans*.

Results

Weakly Voltage-Dependent Conductance

After the addition of a suitable amount of each of the synthetic polypeptides, P20, P15, P10 or P5, to a planar lipid bilayer system an almost immediate increase in membrane conductivity is seen. Steady state is reached within a few minutes following the symmetrical addition of the polypeptides. The conductivity induced is almost voltage-independent at voltages $< \pm 100$ mV, whereas at higher voltages a hyperbolic function of voltage describes the corresponding current/voltage curve. The conductivity, however, is significantly dependent on the concentration of the polypeptides in the aqueous solutions. Plotted on a double-logarithmic scale the conductivity/concentration relation can be fitted in all cases by a straight line, whose slope ranges between 2.2 and 2.5 for the four different polypeptides (data not shown). The concentrations needed to get the same final conductivity are quite different, being higher with the shorter polypeptides, e.g. a conductivity of 5 μS/cm^2 at $V = +50$ mV is reached at 8, 12, 50 and 3000 μg/ml for P20, P15, P10 and P5, respectively.

Table 2. Ion selectivity of voltage-independent conductances induced by polypeptides P20, P15, P10 and alamethicin

Polypeptide	KCl/M *cis*	KCl/M *trans*	f *cis*	f *trans*	V_{rev}/mV	P_{Cl}/P_K
P20	1	0.1	0.62	0.80	35 ± 5	8.2
P15	1	0.1	0.62	0.80	36 ± 4	8.9
P10	1	0.1	0.62	0.80	29 ± 5	5.2
Alamethicin	1	0.1	0.62	0.80	−13 ± 4	0.50

f are activity coefficients of the respective *cis* or *trans* compartment salt solutions taken from Robinson and Stokes (1959). Mean reversal potentials (V_{rev}) ± SD were determined from three different experiments. Permeability ratios were calculated according to the Goldman-Hodgkin-Katz theory. If not otherwise indicated in the text, experimental conditions are the same as in Figs. 1 and 2.

In order to investigate ion selectivity of this weakly voltage-dependent conductance, we measured the reversal potential V_{rev}, i.e., the voltage at which no net current flows across the membrane, if the *cis* compartment is made ten times more concentrated in KCl than the *trans* compartment (*cis:* 1 M, *trans:* 0.1 M). The results of these experiments are listed in Table 2 for P20, P15 and P10. The positive values found for V_{rev} indicate that the weakly voltage-dependent conductance induced by the polypeptides displays anion selectivity. During the course of these experiments large voltage-dependent, long-lived events of step-like conductance changes occasionally appeared. Such events of channel opening and closing will be described in detail in the following. Here we want to mention that ion translocation through these strongly voltage-dependent channels is rather unselective as indicated by a reversal potential of approximately 0 mV, in contrast to that of the weakly voltage-dependent conductance.

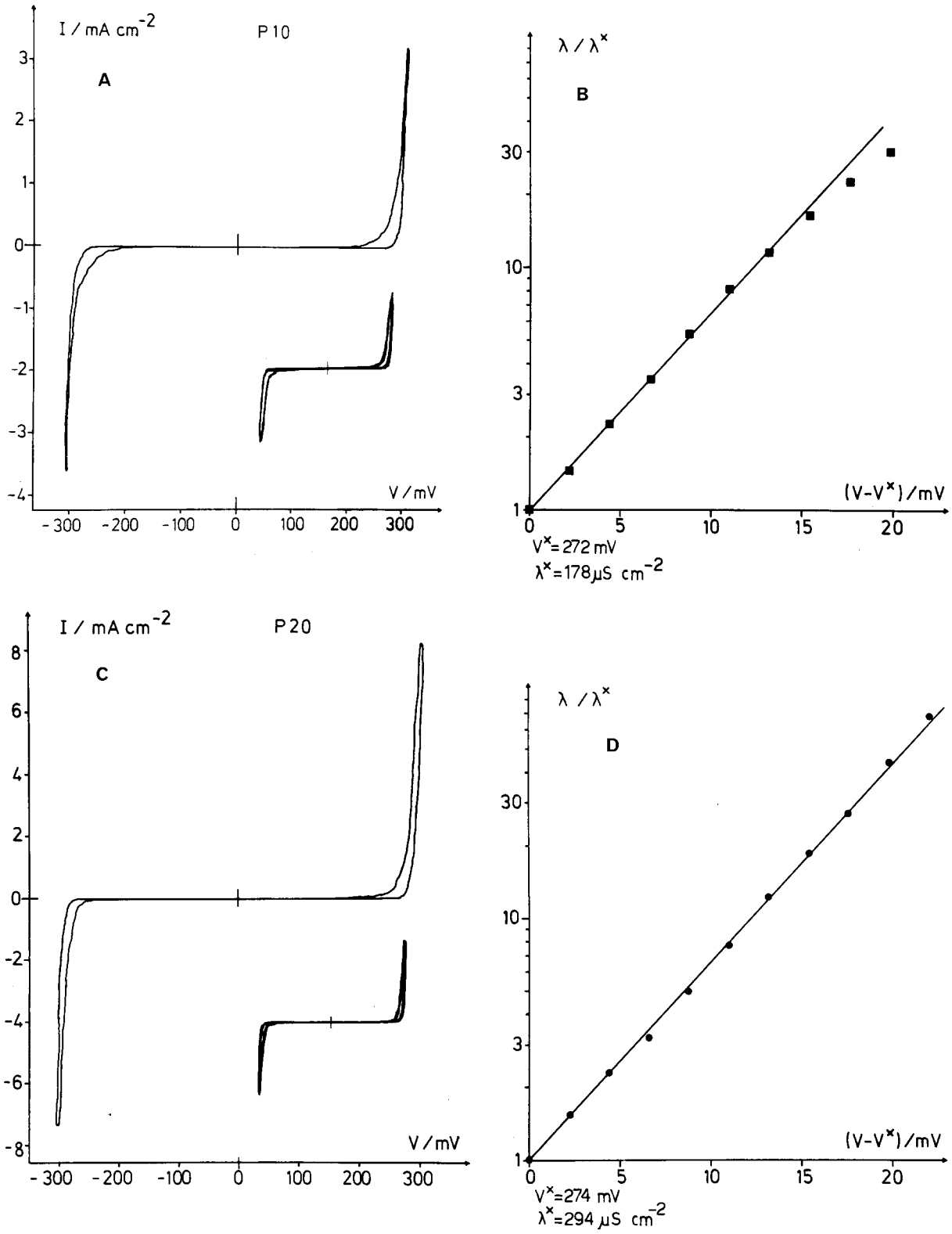

Fig. 1. Current/voltage (I/V) characteristics of the synthetic polypeptides P10 and P20 in planar lipid bilayer membranes. Polypeptides P5 and P15 behave similarly. I/V curves were obtained by applying triangular voltage pulses of 40 sec period time to the bilayer. Examples are shown in *A* (P10) and *C* (P20). In order to demonstrate stationarity of the systems under study three cycles in *A* and five cycles in *C* have been superimposed (shown as insets). Half-logarithmic plots of the corresponding conductivities versus the applied voltages are presented in *B* (P10) and *D* (P20). All experimental points were fitted by straight lines with the same slope of 189 V^{-1}. Saturation, i.e., a decrease in the slope was observed with P5 and P10 at conductivities exceeding 3 mS/cm^2 and with P20 beyond 10 mS/cm^2. P15 exhibited no saturation up to 25 mS/cm^2. Reference voltages V* and reference conductivities λ* for P10 and P20 are given in the diagrams (*B* and *D*). For details *see* text. Experimental conditions: Lipid solution and bilayer forming procedure are described in Materials and Methods. Salt solution—1 M KCl, unbuffered. Polypeptide concentration—*A*:P10—60 μg/ml; *C*: P20—10 μg/ml. Temperature—22–23°C

Alamethicin is known to induce a weakly voltage-dependent conductance in planar bilayers under appropriate conditions, too (Boheim & Kolb, 1978). For comparison, ion selectivity of this type of alamethicin-induced membrane conductivity was measured in a similar way as described above. The weakly voltage-dependent conductance was induced by clamping at a high voltage for a quite long period of time; returning then to low voltages led to the disappearance of the strongly voltage-dependent alamethicin-induced conductance. Only the weakly voltage-dependent conductance was left which slowly decreased in time. The value of the reversal potential thus determined is listed in Table 2, too. Its negative sign indicates cation selectivity, somewhat less pronounced than that reported for the strongly voltage-dependent conductance (Eisenberg et al., 1973).

Strongly Voltage-Dependent Conductance

Current/Voltage (I/V)-Curves

Each of the four synthetic polypeptides, P20, P15, P10 and P5, induce large and strongly voltage-dependent conductances in planar lipid bilayers, if a sufficiently high voltage is applied. This is demonstrated in Fig. 1*A* for P10 and in Fig. 1*C* for P20. The *I/V*-curves were obtained by applying triangular pulses of appropriate amplitude and period time (40 sec) to a membrane after addition of one of the polypeptides to the aqueous salt solution. The current response to a complete voltage sweep cycle is shown: current increases dramatically as soon as a critical value, the so-called switch-on voltage V_c, is reached. For the following we exactly define V_c by the voltage, at which a given polypeptide induces a bilayer conductivity of 100 μS/cm^2. When the applied voltage is reduced, current starts to decrease again. A small hysteresis is observed. Finally, the initial low level of membrane current is adopted. When voltage increases in the opposite direction, the complete curve pattern is reproduced symmetrically. Conditions necessary for this symmetry are: addition of the polypeptide to both compartment solutions bathing the bilayer and sufficient time (ca. one hour) to allow equilibration. Polypeptide addition to only one compartment causes asymmetric *I/V* characteristics. In this case V_c is lower at the positive branch, if the polypeptide is added to the more positive potential side (as observed with alamethicin). The *I/V*-curves for the four different polypeptides are quite similar, also with respect to the small hysteresis. Its reproducibility under fixed experimental conditions is very high. Three *I/V*-cycles are superimposed in Fig. 1*A* and five cycles in Fig. 1*C* in order to demonstrate this fact. The concentrations needed to create these *I/V*-curves are quite different for the polypeptides. The shorter the polypeptide chain, the higher is the concentration for a given switch-on voltage V_c. This type of *I/V*-curves is strongly reminiscent of alamethicin.

In Fig. 1*B* (P10) and *D* (P20) the conductivities induced by the polypeptides concerned are plotted on a logarithmic scale versus the applied voltage. In each case the conductivity is an exponential function of voltage after passing V_c. This equals the well-known behavior of alamethicin. The *I/V* curves of the four polypeptides P5 to P20 were fitted by straight lines with the same slope which reflects an *e*-fold change in conductivity per 5.3 mV. In case of P5 and P10 a decrease in the slope is observed at large induced conductivities ($\lambda_\infty > 3$ mS/cm^2), i.e., the current saturates.

The voltages that have to be applied in order to induce this strongly voltage-dependent conductance ($V > 150$ mV) are unusually high in comparison to those used with alamethicin and its natural analogues. For this reason we repeated the same type of experiments also with alamethicin but at low concentrations of the antibiotic (ca. 50 ng/ml). Under such conditions the switch-on voltage V_c has a magnitude similar to that seen with the synthetic polypeptides. Figure 2*A* shows that the resulting *I/V*-curve is indeed very similar to those presented in Fig. 1. They differ in the extent of the hysteresis. The establishment of a hysteresis is linked to the mean lifetime of channels formed, as it will become clear in the following.

Similar experiments have been carried out with the natural hexadecapeptide antibiotic antiamoebin. It is only remotely related to alamethicin. Its sequence includes besides the α,α-dialkylated amino acids (Aib, Iva) and phenylalaninol (Pheol) two hydroxyproline residues. The *I/V*-curve in Fig. 2*B* shows a somewhat different pattern. After reaching a characteristic switch-on voltage V_c membrane current starts to increase and it continues to increase even if the voltage is already reduced. This fact explains the negative slope of the rising phase of the *I/V*-curve in Fig. 2*B*. When the voltage is further reduced, the antiamoebin-induced current starts to decrease again and finally attains bare membrane level. Attempts to continuously increase membrane voltage, when V_c was reached, usually led to membrane breakdown. For this reason it is not possible to draw a conductivity/voltage plot as in cases of P5 to P20 (Fig. 1). However, it is quite easy to determine V_c in its dependence on experimental parameters.

A common feature of the *I/V*-curves presented above is that V_c depends on the aqueous polypeptide concentration. When this concentration is increased, V_c decreases (Fig. 3). V_c is plotted versus the concentration of the six different polypeptides

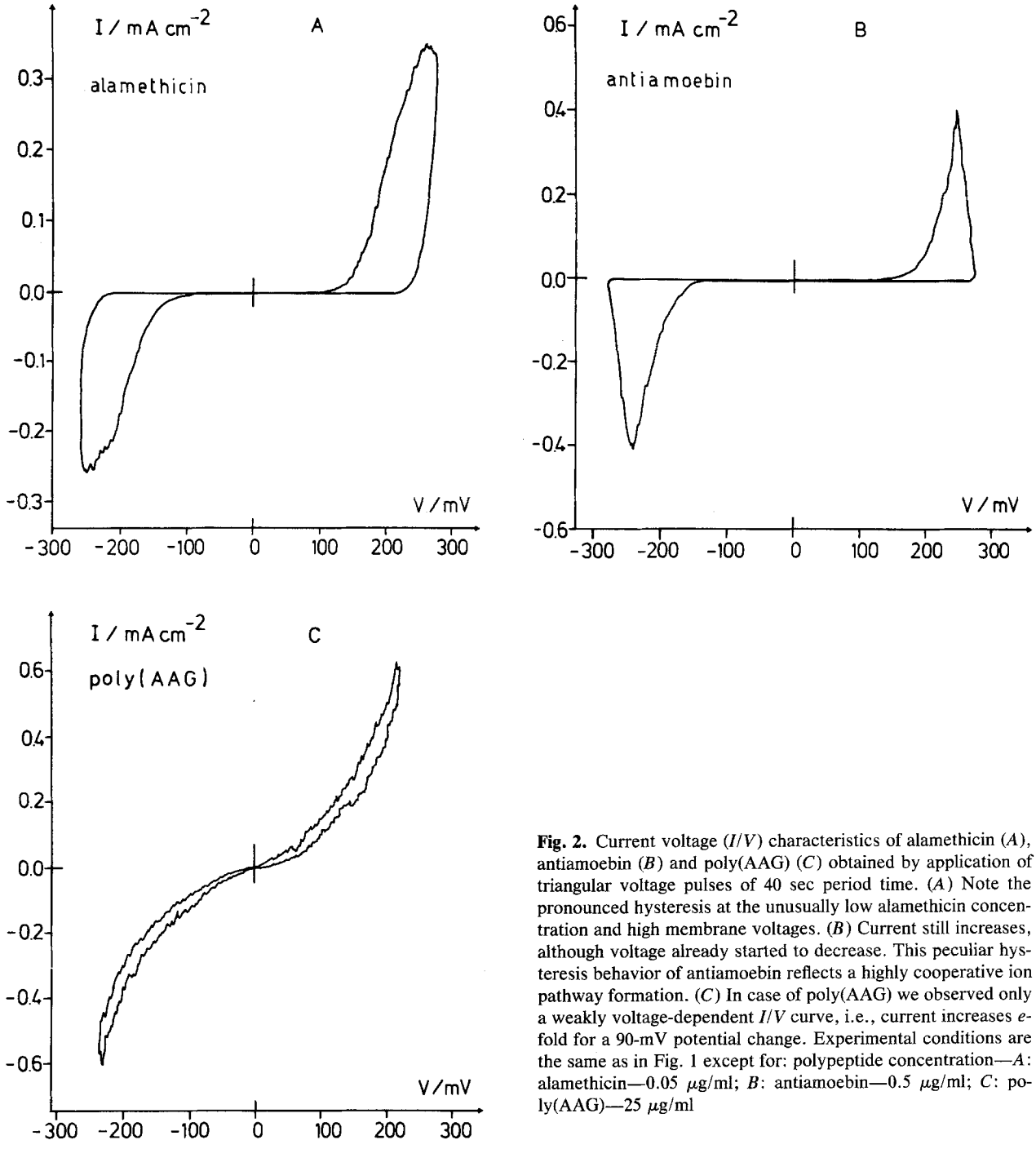

Fig. 2. Current voltage (I/V) characteristics of alamethicin (A), antiamoebin (B) and poly(AAG) (C) obtained by application of triangular voltage pulses of 40 sec period time. (A) Note the pronounced hysteresis at the unusually low alamethicin concentration and high membrane voltages. (B) Current still increases, although voltage already started to decrease. This peculiar hysteresis behavior of antiamoebin reflects a highly cooperative ion pathway formation. (C) In case of poly(AAG) we observed only a weakly voltage-dependent I/V curve, i.e., current increases e-fold for a 90-mV potential change. Experimental conditions are the same as in Fig. 1 except for: polypeptide concentration—A: alamethicin—0.05 μg/ml; B: antiamoebin—0.5 μg/ml; C: poly(AAG)—25 μg/ml

on half-logarithmic scale (Fig. 3). Experimental points are fitted by straight lines and their slopes are identical in all cases, corresponding to a 102-mV shift in V_c for a tenfold change of polypeptide concentration. It should be noted, however, that the concentration needed to reach a given value of V_c turns out to be significantly different from one polypeptide to the other. The natural antibiotics are more potent than the synthetic peptides. Alamethicin is the most effective one and among the synthetic polypeptides the activity is higher the longer its chain length.

The conductance-inducing effects of the short-chained P5 were particularly surprising. For this reason we tested two other short-chained polypeptides: the synthetic 3_{10}-helical pentapeptide P5a and the C-terminal hexapeptide fragment of trichotoxin TT 13–18 (*see* Table 1). Both polypeptides yielded

I/V-curves similar to those presented in Fig. 1. Furthermore, V_c values were comparable, i.e., P5a: 280 mV at 0.5 mg/ml; TT 13–18: 300 mV at 0.25 mg/ml. Recently, the crystal structures of the two polypeptides P9 and P11 (*see* Table 1) were found to be mainly α-helical. We measured the conductance-inducing properties of P9 and P11 in planar bilayers. Data were very similar to those reported for P10.

Previously it was shown by Urry et al. (1978) that the synthetic polypeptide HCO-(L-Ala-L-Ala-Gly)$_5$-OMe forms voltage-dependent transmembrane channels in planar bilayers. Due to structural model considerations it was supposed that a β-helical channel similar to that of gramicidin A may have formed (Urry et al., 1978). We wanted to know if the voltage-dependence of channel formation by this polypeptide resembles that observed with alamethicin and the structurally related peptides P5 to P20. A series of experiments was carried out with a mixture of similar polypeptides, labeled poly(AAG) (*see* Table 1). A typical *I/V*-curve obtained with poly(AAG) under experimental conditions otherwise identical to those used with P5 to P20 (Fig. 1) is shown in Fig. 2*C*. A comparison of the various *I/V*-characteristics reveals that the conductivity induced by poly(AAG) is indeed voltage-dependent but significantly less pronounced than with P5 to P20. The conductivity increases only *e*-fold per 90-mV change of the applied voltage. Results are in good agreement with those reported by Urry et al. (1978) and thus suggest a channel formation mechanism for poly(AAG) different from that for P5 to P20 and alamethicin.

Finally, we considered the possibility that the polypeptide induced current could arise from a detergent-like action on the lipid bilayer. Therefore, we studied the voltage-dependent effects of the detergent sodium dodecylsulfate (SDS) on planar bilayers. We observed current fluctuations at high voltages in the presence of SDS, but it was not possible to record a complete *I/V*-curve under experimental conditions given in Figs. 1 and 2. Attempts to reach conductivities larger than 100 μS/cm^2 always led to membrane breakdown. In sharp contrast, conductivities up to 20 mS/cm^2, i.e., larger by at least two orders of magnitude, could be easily achieved in the presence of P5 to P20.

Voltage-Jump Current-Relaxation Experiments

Another useful technique to obtain information about the mechanism of channel formation by alamethicin and its analogues is the study of the time course of current relaxations which follow the application of voltage-jumps to doped membranes. These data are complementary to those derived

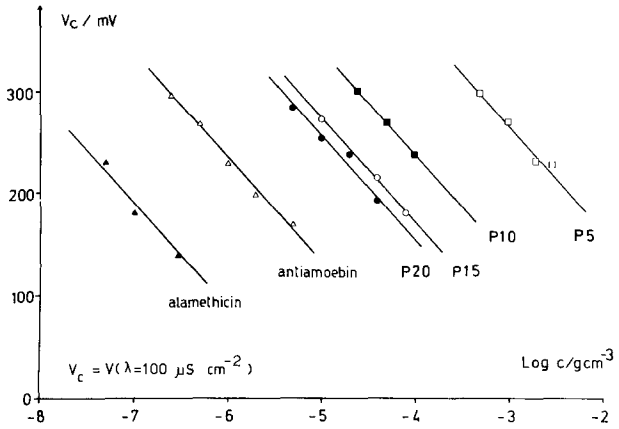

Fig. 3. Dependence of the switch-on voltage V_c on the concentration of a variety of polypeptides: alamethicin, antiamoebin, P20, P15, P10 and P5. V_c is defined by the voltage, at which a polypeptide-induced conductivity of 100 μS/cm^2 is reached. Experimental points for each polypeptide were fitted in a half-logarithmic plot by straight lines with the same slope, which corresponds to a decrease of 101.8 mV in V_c for a tenfold increase in concentration. Experimental conditions are otherwise the same as in Figs. 1 and 2

from *I/V*-characteristics. The results of applying voltage square pulses to membranes modified by either alamethicin or P20 are shown for comparison in Fig. 4*A-C*. In case of alamethicin, all the current, which had been induced by this antibiotic at a distinct voltage, abruptly disappears after voltage-sign reversal. Then the current increases in an exponential way towards the new steady state. The same behavior is observed upon the opposite voltage change (Fig. 4*A*). This is different with P20 (Fig. 4*B*), which is representative also for the other shorter polypeptides. Here, the P20 induced current does not disappear completely upon voltage-sign reversal. Most of the current is left and only a current relaxation of small amplitude is observed. However, if the applied voltage is clamped to 0 mV for a short period of time, then after application of the new voltage a current relaxation of large amplitude is recorded, because the previously induced current had vanished completely (Fig. 4*C*).

We tried to characterize the behavior of alamethicin at the unusually high voltages used for recording the *I/V* curves presented above, i.e., we made experiments at low antibiotic concentrations. Two current-relaxation curves, which led approximately to the same steady-state current, were obtained at two sets of different but complementary voltages and alamethicin concentrations (Fig. 5*A* and *B*). At the higher concentration, i.e., lower applied voltage, the time course of the relaxation trace can be fitted by a single exponential function (in

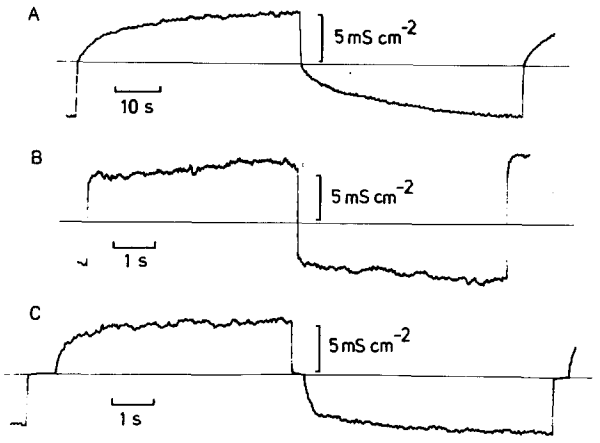

Fig. 4. Voltage-jump current-relaxation experiments in the presence of alamethicin (*A*) and P20 (*B* and *C*). (A) A square wave of 0.01 Hz frequency, which jumped between +202 and −195 mV, was applied at an alamethicin concentration of 0.06 μg/ml. After each voltage change the alamethicin-induced conductance immediately dropped to the bare membrane level and then increased exponentially towards the steady state. (*B*) The same procedure was used with the P20-modified bilayer, applying a square wave of 0.1 Hz frequency and voltages between +247 and −237 mV. P20 concentration was 20 μg/ml. In contrast to the behavior with alamethicin most of the polypeptide-induced conductance survived the voltage change. (*C*) Conditions are the same as in *B*. However, voltage jumps between +244 and −234 mV were interrupted by a short-lasting intermission at 0 mV. This short stay at zero voltage was sufficient to destroy all the P20-induced conductance, because thereafter current relaxation occurred exponentially from the bare membrane level to its steady state. A small voltage offset was used with all traces above in order to reach the same final current at positive and negative voltages. Experimental conditions are otherwise the same as in Figs. 1 and 2

TABLE 3. Dependence of time constants τ_s and τ_s^* in voltage-jump current-relaxation experiments on alamethicin concentration and final voltage V^a

Alamethicin (μg/ml)	V (mV)	λ_∞ (mS/cm^2)	τ_s (sec)	τ_s^* (sec)
0.500	86	25.7	0.40	—
0.250	119	25.1	0.48	—
0.125	172	24.9	3.10	0.48
0.062	220	23.9	18.44	1.95

[a] Data are referred to a constant steady-state conductivity of λ_∞ = 24–26 mS/cm^2. Experimental conditions are the same as in Fig. 5.

agreement with published results (Boheim & Kolb, 1978)) with a time constant of τ = 0.48 sec (Fig. 5*A*). In contrast, at the lower concentration, i.e., at the higher voltage, the time course of the current relaxation can be sufficiently described only by the sum of two exponential functions of time constants τ_s = 18.4 sec and τ_s^* = 1.95 sec (Fig. 5*B*). In Table 3 a set of time constants is listed which were measured at four different alamethicin concentrations but almost the same final current. In order to achieve this current normalization an appropriate set of quite different voltages had to be applied. It is seen that the time constants increase with decreasing antibiotic concentration (and increasing membrane voltage) and that at sufficiently low concentrations two exponential components appear. The corresponding time constants differ almost by a factor of ten.

The same procedure was used with membranes modified by the polypeptides P20, P15, P10 and P5 (Table 4). As shown in Fig. 5*C* (P20) and *D* (P10) the time course of current relaxations can only be described by the sum of two exponential functions, the time constants of which differ by about one order of magnitude. This is similar to the situation with alamethicin at low concentrations. At a fixed peptide concentration both time constants, τ_s and τ_s^*, depend on the applied voltage, i.e., concomitantly on the final value of the bilayer current. This is shown in detail in Fig. 6*A* and *B*. In a double-logarithmic plot two sets of time constants are presented in their dependence on the steady-state conductivities which were measured with alamethicin, P20 and P10, respectively. Experimental points can be fitted by straight lines with negative slopes. Steeper slopes are found with the synthetic polypeptides than with alamethicin. A negative slope dependence is unusual for alamethicin. Boheim and Kolb (1978) reported that, at constant alamethicin concentration, the (slow) time constant of current relaxations becomes larger towards increasing applied voltages and hence towards increasing final conductivities. This means that the slope is positive in a τ_s/λ_∞ plot. The variation in behavior is explained by the different voltage ranges used: ≲100 mV (Boheim & Kolb, 1978), >150 mV (this study). At the high voltages applied and correspondingly low concentration alamethicin behaves similarly to the synthetic polypeptides. Control experiments at an alamethicin concentration twice that of Fig. 6*A* and *B* revealed that already under these conditions both time constants increase with the final conductance (*data not shown*).

Since the relaxation curves with alamethicin, P20 and P10 at high voltages are described by the sum of two exponential functions, it is interesting to look at the dependence of the corresponding current amplitudes on the final conductivity. In Fig. 6*C* the ratio of the amplitude of the slower process A_s to that of the faster process A_s^* is plotted versus the final conductivity on double-logarithmic scale. Straight lines with negative slope fit the data,

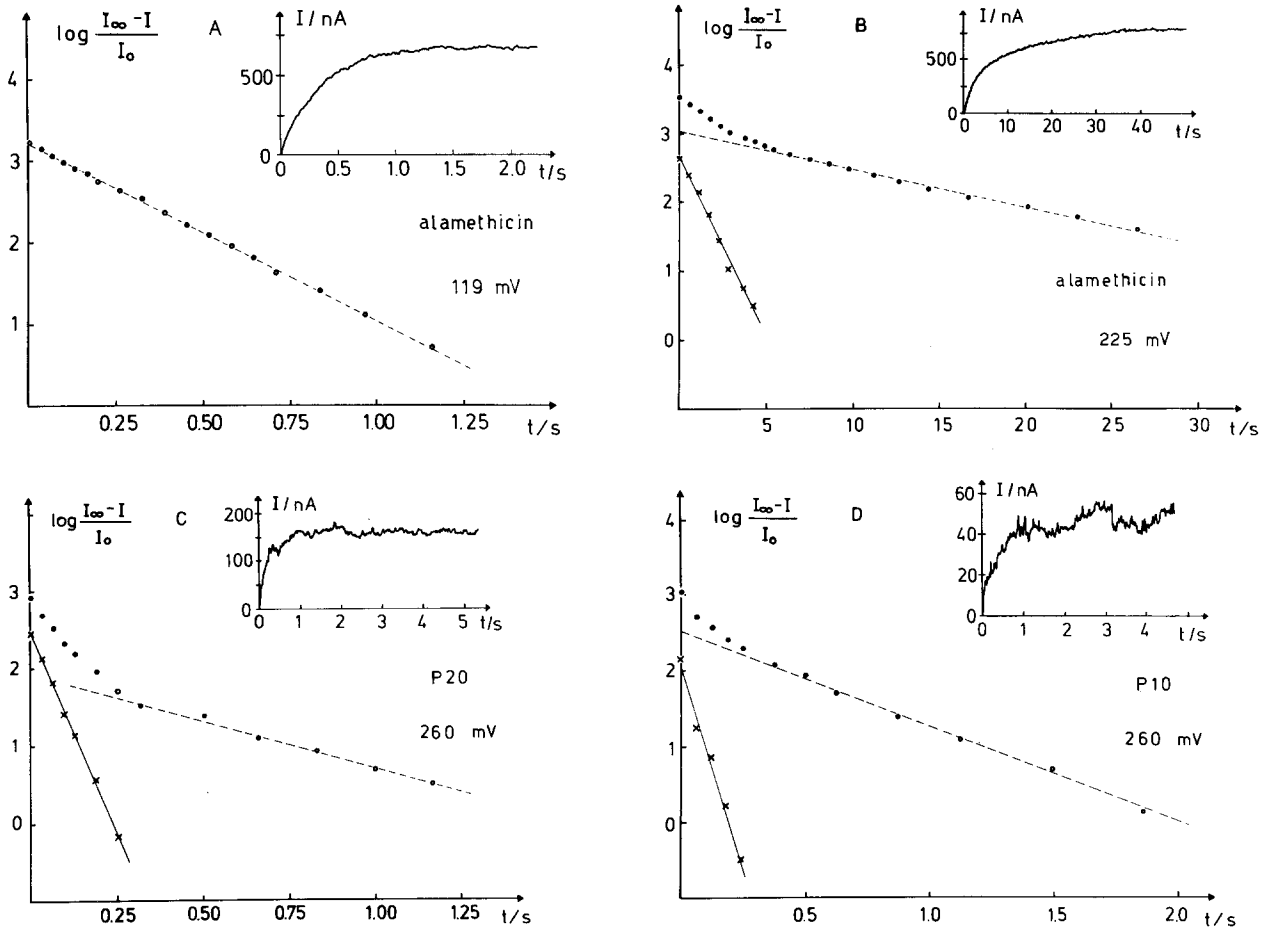

Fig. 5. Time course of current relaxations in voltage-jump experiments in the presence of alamethicin (*A, B*), P20 (*C*) and P10 (*D*). In each drawing the current versus time curve is presented as inset, whereas its corresponding digitized trace is plotted on half-logarithmic scale. For this plot arbitrary units were used by dividing the relaxation amplitude at each time by a convenient reference current I_o. Voltage-jumps occurred from 0 mV to the final voltage given below. (*A*) Least squares fit reveals a single time constant τ = 0.48 sec. Alamethicin concentration: 0.25 μg/ml; applied voltage: +119 mV; I_o = 25 nA. (*B*) At low alamethicin concentration, c = 0.06 μg/ml, and high membrane voltage, V = +225 mV, the current-relaxation curve can only be fitted by the sum of two exponential functions. By least squares fitting a slow time constant of τ_s = 18.4 sec and after subtraction of the slow component another faster time constant of τ_s^* = 1.95 sec were obtained. I_o = 25 nA. (*C*) Current relaxations in the presence of P20 reveal that two exponential components have to be considered here, too. P20 concentration was 20 μg/ml, applied voltage V = +260 mV and I_o = 10 nA. Least squares fitting of the two time constants yields τ_s = 0.82 sec and τ_s^* = 0.098 sec, respectively, which are both considerably faster than those obtained with alamethicin. (*D*) A similar behavior is observed with P10 at a concentration of 100 μg/ml, an applied voltage of + 260 mV and I_o = 2.5 nA. The two time constants are: τ_s = 0.8 sec and τ_s^* = 0.096 sec. Experimental conditions are the same as in Fig. 4

whereby slopes are similar with P20 and P10 but again steeper than in the presence of alamethicin. The negative slope implies that the faster process becomes more probable towards higher voltages. Data shown in Fig. 6 are representative also for P15, P5 and the other related polypeptides. Similar straight lines and parameter interrelations were obtained. When we compare the time constants obtained with different polypeptides at the same final conductivity and approximately the same applied voltage, it becomes visible (Table 4) that both time constants, τ_s and τ_s^*, decrease in the sequence alamethicin > P20 > P15 > P10. The shorter the polypeptide chain, the faster is its relaxation into the new steady state. It should be noted that P10 and P5 exhibit almost the same values of time constants under the given conditions.

At high values of the final conductivity ($\lambda_\infty > 5$ mS/cm²) two additional features in the current-relaxation behavior emerge (Fig. 7). First, a delay in current increase of less than 10 msec occurs after the voltage jump (Fig. 7*A*). Second, one observes a decrease of the final conductivity after having passed a maximum value. Both delay and inactiva-

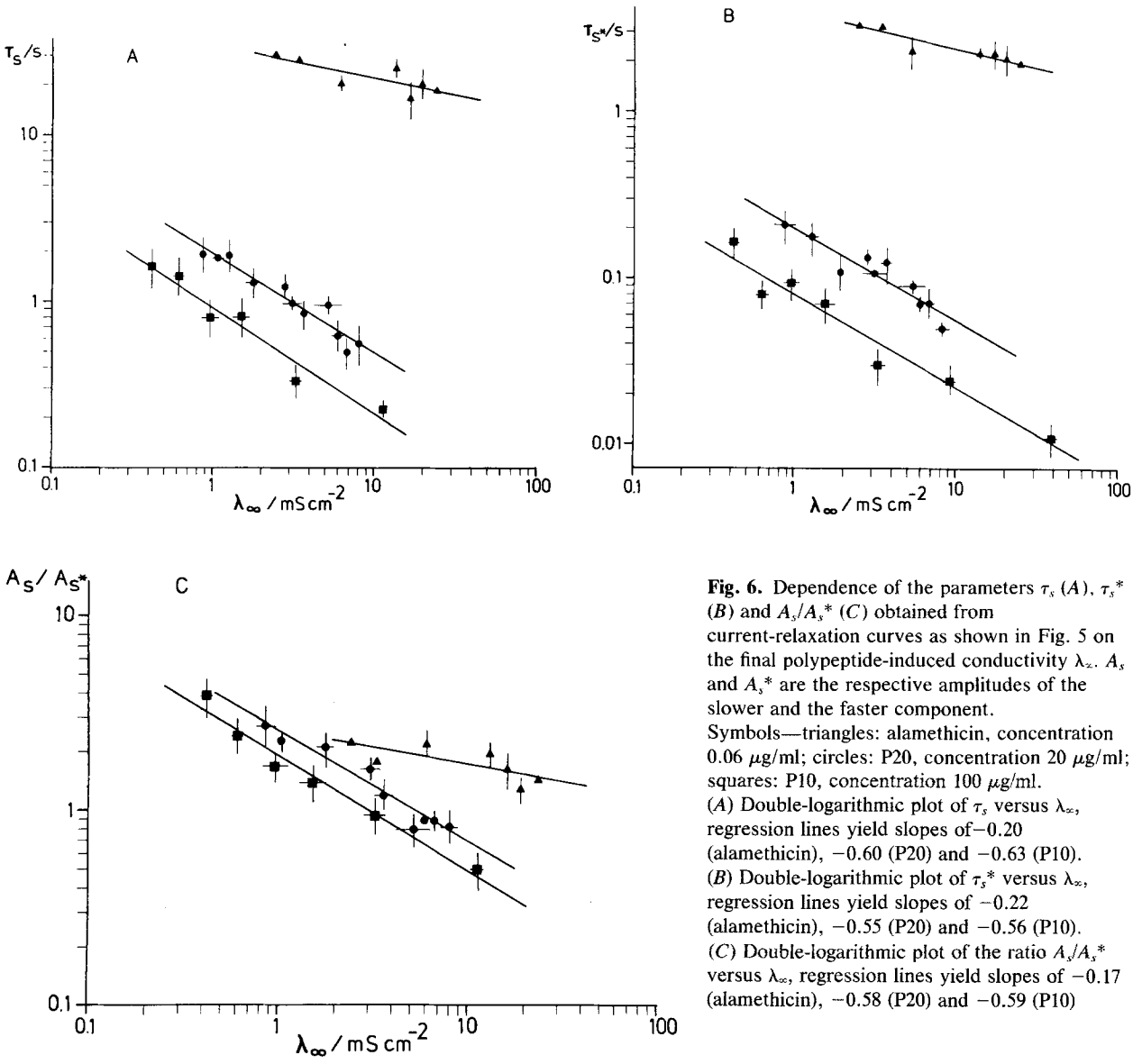

Fig. 6. Dependence of the parameters τ_s (*A*), τ_s* (*B*) and A_s/A_s* (*C*) obtained from current-relaxation curves as shown in Fig. 5 on the final polypeptide-induced conductivity λ_∞. A_s and A_s* are the respective amplitudes of the slower and the faster component. Symbols—triangles: alamethicin, concentration 0.06 μg/ml; circles: P20, concentration 20 μg/ml; squares: P10, concentration 100 μg/ml. (*A*) Double-logarithmic plot of τ_s versus λ_∞, regression lines yield slopes of −0.20 (alamethicin), −0.60 (P20) and −0.63 (P10). (*B*) Double-logarithmic plot of τ_s* versus λ_∞, regression lines yield slopes of −0.22 (alamethicin), −0.55 (P20) and −0.56 (P10). (*C*) Double-logarithmic plot of the ratio A_s/A_s* versus λ_∞, regression lines yield slopes of −0.17 (alamethicin), −0.58 (P20) and −0.59 (P10)

tion behavior have been reported for alamethicin, too (Mueller, 1976; Boheim & Kolb, 1978). They are particularly evident with P10 and P5. The exponential-like time course of the inactivation process is significantly slower than the slow process of current activation described by τ_s.

Single Channel Current Fluctuations

It is well known from studies of alamethicin and its natural analogues that discrete conductance fluctuations may be observed, if the membrane is clamped at a constant voltage somewhat below the characteristic switch-on voltage. These stepwise current changing events are due to the formation of single ionic channels within the lipid bilayer. The alamethicin channel typically exhibits a number of nonintegral conductance levels which are adopted in strict sequence. In order to gain insight into the elementary mechanism of voltage-dependent conductance increase by the synthetic polypeptides we used this technique.

After application of a suitable membrane voltage, discrete current fluctuations are observed with all synthetic polypeptides. By way of example, this is shown for P5 and P15 in Fig. 8*A* and *C*, respectively. The conductance fluctuation amplitudes are large, in the range of several nS. They may result from the formation of wide transmembrane water-containing channels. Single channel current events are similar for the four polypeptides but signifi-

Table 4. Time constants τ_s and τ_s^* of polypeptide-induced current relaxations in voltage-jump experiments as referred to a constant steady-state conductivity of λ_∞ = 2.8–3.3 mS/cm²[a]

Polypeptide	c (μg/ml)	V (mV)	λ_∞ (mS/cm²)	τ_s (sec)	τ_s^* (sec)
Alamethicin	0.06	192	3.2	27.9	3.25
P20	20	250	2.8	1.2	0.134
P15	50	240	2.9	0.84	0.085
P10	100	270	3.3	0.33	0.030
P5	2000	282	2.9	0.32	0.028

[a] Experimental conditions are the same as in Fig. 5.

Table 5. Mean conductance values $\bar{\Lambda}$ of single polypeptide channels[a]

Polypeptide	$\bar{\Omega}$ (nS)	l[d] (Å)	$\bar{\Lambda} \cdot 1$ (nS · Å)	$\bar{\Lambda} \cdot 21$ (nS · Å)
Alamethicin	5.1 ± 1.3[b]	32	163.2	—
P20	6.2 ± 0.3 (6)[c]	30	186	—
P15	7.6 ± 0.3 (5)	22.5	171	—
P10	11.2 ± 0.1 (2)	15	168	—
P5	10.7 ± 0.5 (4)	7.5–10	80.2–107	160.5–214

[a] Experimental conditions are the same as in Fig. 8.
[b] Mean conductance of the most probable pore state level ±1 for alamethicin as evaluated from Fig. 10.
[c] In case of P5 to P20 number of experiments is given in parentheses.
[d] Length of polypeptide chains as obtained from crystallographic data (Fox & Richards, 1982; Bosch, 1984). For details *see* text.

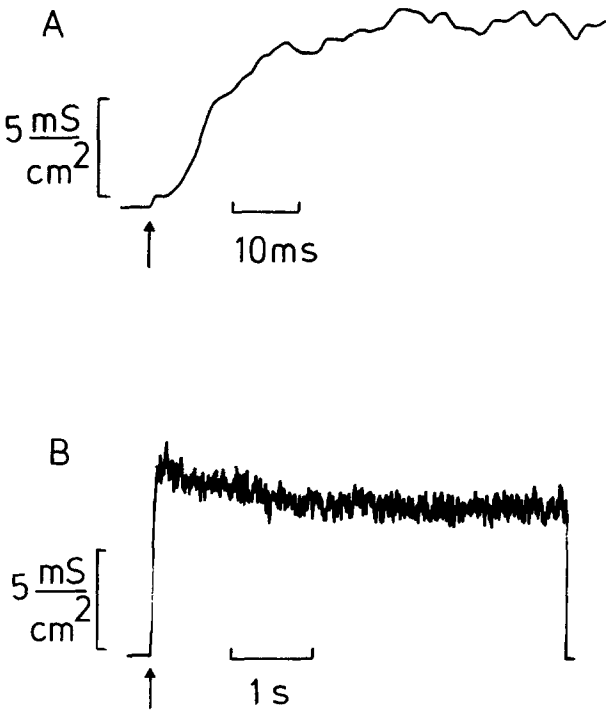

Fig. 7. Time course of current relaxations after voltage jumps (from 0 to +280 mV) in the presence of P10 (concentration 100 μg/ml). Arrows point at the time of voltage change. The initial part of trace *B* is shown in *A* at an enlarged time scale. (*A*) Delay period—After the voltage-jump membrane current increased with an *S*-shaped time-course. The time delay lies in the msec range. Initial current is determined by the value of the weakly voltage-dependent conductance at 0 mV. (*B*) Inactivation—After passing a maximum, membrane current slowly decreases in an exponential-like decay. The corresponding time constant of inactivation is orders of magnitude larger than that of the activation process. Experimental conditions are the same as in Fig. 4

cantly different from the corresponding fluctuation pattern of alamethicin. This is concluded from conductance histograms drawn in Fig. 8*B* (P5) and *D* (P15), which reveal a relatively broad conductance distribution with a single maximum in contrast to several maxima seen in distributions of alamethicin channels (Boheim, 1974). Comparing the respective maxima of polypeptide conductance distributions (Table 5), one concludes that the larger mean conductance values are found with the shorter molecules. P5 and P10 have similar mean conductances, while mean P20 conductance is about half that size and the P15 conductance maximum lies in between. Channel lifetimes are longer the longer the polypeptide chain.

In addition to these relatively short-lived events sometimes current changes of extremely long duration occur. Examples of onsets of such long-lived events are indicated by arrows in Fig. 8*A* and *C*. The probability of observing long-lived events seems to be higher at low voltages. This is shown in Fig. 9, where all three techniques discussed in this paper are applied to the same membrane doped with P20, i.e., *I/V*-characteristic (Fig. 9*A*), single channel current fluctuations near V_c (Fig. 9*B*), and voltage-jump current relaxation curves (Fig. 9*C* and *D*). The single channel trace reveals both long-lived events, which are indicated by arrows, and short-lived channels (Fig. 9*B*). The *I/V*-curve, which is shown at an enlarged scale in Fig. 9*A*, indicates that long-lived channels are present mainly at the very beginning of the rising phase, whereas fast current fluctuations become more important at higher voltages. This fact is demonstrated even more clearly by the voltage-jump experiments (Fig. 9*C* and *D*). The current-relaxation curve at the lower voltage (225 mV) is composed of mainly long lasting steps, whereas that curve at the higher voltage (265 mV) shows fast fluctuations which reflect the superposition of short-lived channel currents.

At first sight all fluctuation events presented in Fig. 8 for the various polypeptides appear to be on-off transitions between an open channel conduc-

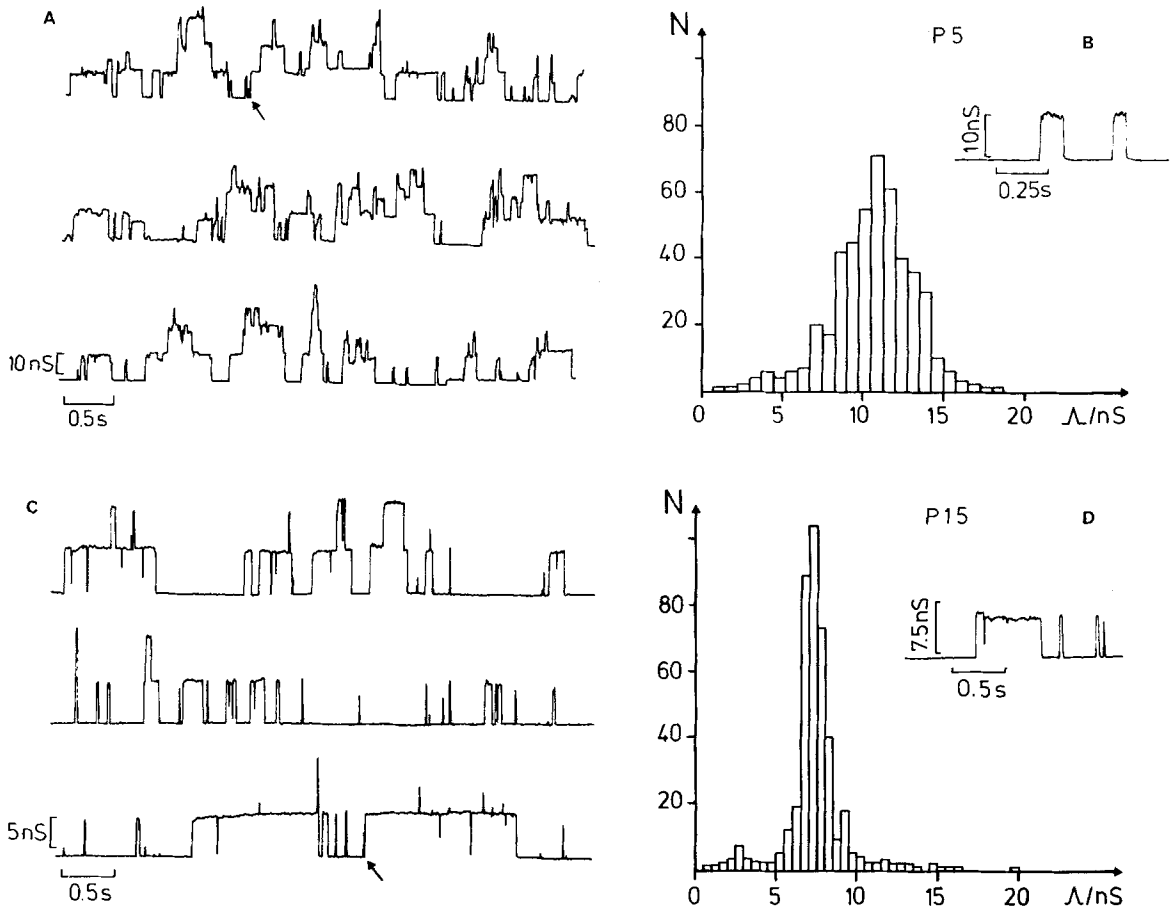

Fig. 8. Single channel current fluctuations at constant applied voltage (*A*, *C*) and the corresponding conductance distributions (*B*, *D*) in planar bilayers modified by the polypeptides P5 and P15. Corresponding results are obtained with P10 and P20. (*A*, *B*) P5—concentration 2 mg/ml; applied voltage +258 mV; 471 events from four different experiments. (*C*, *D*) P15—concentration 20 μg/ml; applied voltage +268 mV; 421 events from five different experiments. Increase in polypeptide chain length leads to a decrease of the mean channel conductance and to an increase of its mean lifetime. With all four peptides occasionally channels of particularly long lifetime appear; examples are indicated by arrows in *A* and *C*. Open channel levels display a significantly increased current noise as compared to that of the bare membrane level; examples of such fluctuation traces are shown as insets in *B* and *D*. Experimental conditions are otherwise the same as in Fig. 1

tance level and the bare membrane level. The open channel current noise is, however, considerably larger than that of the bare membrane current. This increased noise amplitude results from transitions between the most probable conductance level and some discrete adjacent levels. Examples of such noise traces are shown in Fig. 8*B* and *D* as insets. In order to resolve these current fluctuations between open channel levels we carried out experiments at reduced temperature by cooling the membrane down to 5°C, which was still sufficiently above the main phase transition temperature of the membrane lipid. By slowing down channel-gating kinetics it was possible to resolve more clearly step-like fluctuations between adjacent current levels. Examples are given in Fig. 10*A* for P20 and *B* for P10. Sometimes current transitions do not display a rectangular shape up to the final current level. This may reflect a slow drift in the time-averaged size of the channel aggregate. We want to emphasize the notion that all these phenomena of single channel current fluctuations are observed as well with the other related polypeptides P11, P9, P5a and TT 13–18. At the high voltages considered antiamoebin behaves similarly, too.

Finally, we also studied alamethicin single channel current fluctuations at high applied voltages. Figure 10*C* and *D* demonstrate that an almost tenfold decrease in alamethicin concentration, which is compensated by a concomitant increase of the membrane voltage by about 100 mV needed to observe single channel current fluctuations, significantly changes the fluctuation pattern. A strong increase of both the lifetime of single level events as

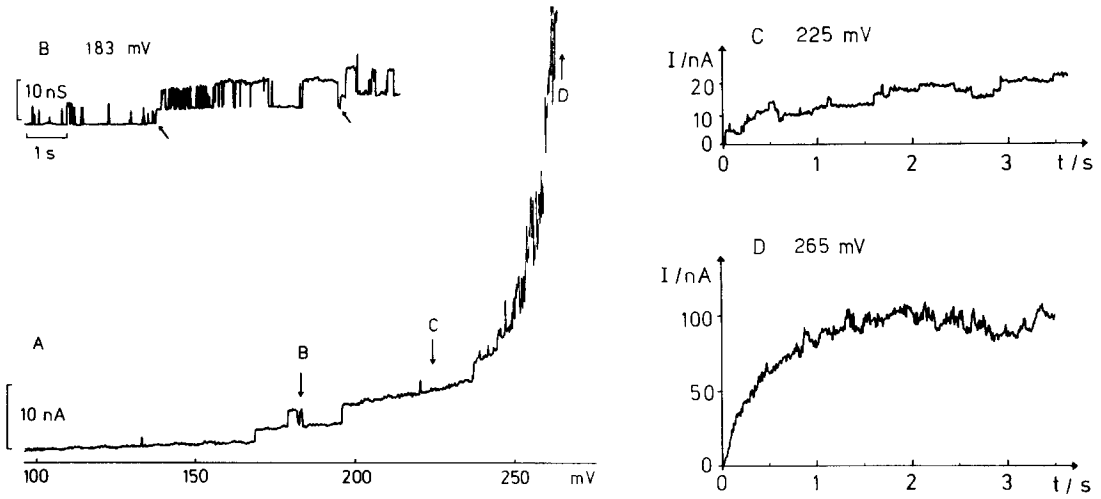

Fig. 9. Voltage dependence of the probability of observing long-lived channels; P20 concentration: 20 μg/ml. (*A*) *I/V* curve at an enlarged voltage scale within the range on the switch-on voltage. Rate of voltage increase was 25 mV/sec. Current steps due to the opening of single channels can be clearly detected. These events are mainly long lived at low but become short-lived at higher voltages. (*B*) Voltage-clamp experiment at +183 mV near the switch-on voltage. Both, long- and short-lived channel types coexist. The onset of long-lasting events is indicated by arrows. (*C*) Current-relaxation curve after a voltage-jump from 0 to +225 mV. Long-lived events are preferred, and the relaxation time constant is large. (*D*) Current relaxation as above but after a voltage jump from 0 to +265 mV. Fast events mainly occur in this case, and the relaxation time constant turns out to be shorter. The constant voltages, at which we recorded the three traces *B*, *C* and *D*, are indicated by arrows on the *I/V*-curve in *A*. Experimental conditions are the same as in Fig. 8

well as that of complete channel bursts occurs towards high voltages. Whereas at 102 mV (Fig. 10*C*) burst fluctuations are similar to those published earlier (Eisenberg et al., 1973), those at 218 mV (Fig. 10*D*) exhibit current steps of extremely long duration comparable to observations of long-lived events with the polypeptides. This increase in the lifetime of alamethicin channels is in good agreement with the two observations mentioned above. First, the time constants of current relaxations become much larger towards decreasing alamethicin concentrations and complementary increased voltages (Table 3, Fig. 5*A* and *B*). Second, the hysteresis observed in *I/V* curves is strongly expressed at low antibiotic concentrations (Fig. 2*A*).

Discussion

Weakly Voltage-Dependent Conductance

Spectroscopic studies indicated that the synthetic polypeptides P20, P15, P10 and P11 used in this study adopt α-helical conformation either in organic solvents or in the crystallized state (Jung et al., 1983*c*; Bosch et al., 1985*a*). The other polypeptides P9, P5, P5a and TT 13–18 also possess ordered structures. Whereas P9 adopts a mixed $\alpha/3_{10}$-helix, the short-chained peptides presumably form 3_{10}-helices as found for P5a in the crystalline state (Bosch et al., 1984). Since all these sequences are entirely hydrophobic, they are expected to incorporate spontaneously into the lipid membrane. Indeed, when we added the synthetic polypeptides to the bilayer bathing solutions, a large voltage-independent or, respectively, weakly voltage-dependent membrane conductance developed. With the four polypeptides studied in detail, P20, P15, P10 and P5, this conductance shows a roughly 2nd power dependence on the polypeptide concentration in 1 M salt solution. This behavior is strongly reminiscent of that reported on alamethicin, since this natural polypeptide antibiotic induces a weakly voltage-dependent conductance in planar bilayers, too (Roy, 1975; Boheim & Kolb, 1978), which has the same power dependence on peptide concentration. We conclude that the weakly voltage-dependent conductance induced by the synthetic polypeptides as well as by alamethicin results from the same membrane-modifying mechanism.

A peculiar property of α-helices is their dipole moment which corresponds to the dipole moment of two half-elementary charges of opposite sign placed at the ends of the helix (Hol et al., 1981; Hol, 1985). Similar considerations apply to the 3_{10}-helix. Therefore, the insertion of helical polypeptides into lipid bilayers is mainly determined by the electric field within the membrane as well as by electrostatic interaction between the dipolar molecules themselves. Added to one side of the bilayer, helical rods

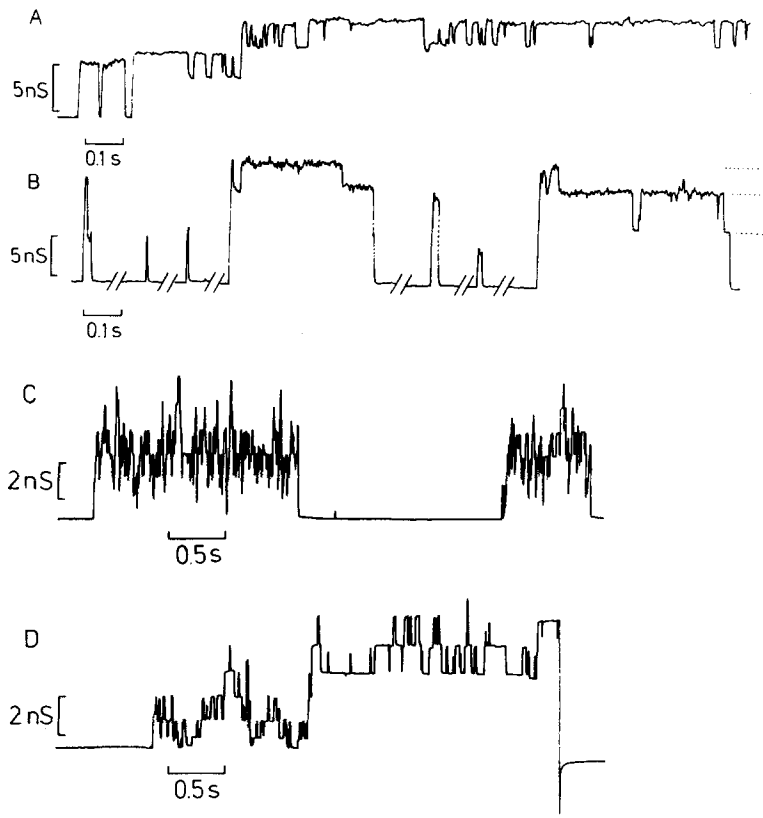

Fig. 10. Single channel current fluctuations of P20 (*A*), P10 (*B*) at low temperature (5°C) and alamethicin (*C*, *D*) at room temperature. (*A*) P20 concentration 10 μg/ml; applied voltage +237 mV; (*B*) P10 concentration 40 μg/ml; applied voltage +256 mV. The long intervals at bare membrane level in *B* were shortened for a clearer presentation; the complete trace lasted about 10 sec. Spontaneous transitions between different conductance levels of single channels were observed at this low temperature for the synthetic polypeptides. Three distinct levels are marked by arrowheads in *B*. (*C*) Alamethicin concentration 0.5 μg/ml; applied voltage +102 mV; (*D*) Alamethicin concentration 0.06 μg/ml; applied voltage 218 mV. Both lifetimes of each conductance level as well as that of the channel itself are considerably increased at the lower concentration. In *D* the particular channel became stabilized between the 5. and 7. conductance level according to the normal conductance sequence. It was arbitrarily destroyed at the end of the trace by reversing the applied voltage. Experimental conditions are the same as in Fig. 8

may insert as monomers with orientation perpendicular to the membrane plane and subsequently form dimers in antiparallel array, because some of the flexible small molecules may undergo spontaneous transversal reorientation (flip-flop movement). Such a mechanism has been proposed for alamethicin (Boheim et al., 1983), which exhibits a large intrinsic dipole moment (Schwarz & Savko, 1982; Yantorno et al., 1982). If polypeptides are added to both sides of a planar bilayer, the spontaneous establishment of larger aggregates of antiparallel oriented dimers seems to be energetically favored. In terms of thermodynamics this behavior corresponds to the formation of separated phases, because polypeptides and membrane lipids seem not to be completely miscible. The existence of such a separated alamethicin-rich phase within a lipid matrix was inferred from measurements near the main phase transition temperature of the membrane lipid (Boheim, Hanke, Überschär & Eibl, 1982) and from electron microscopic investigations (McIntosh, Ting-Beall & Zampighi, 1982).

We suppose that the weakly voltage-dependent conductance may result from the passage of ions through space between neighboring helical rods which constitute these aggregates of oligomeric size, e.g., dodecamers (*see below*). The 2nd power dependence on polypeptide concentration measured would then indicate that the antiparallel dimer might be the particular unit which is primarily responsible for the appearance of this weakly voltage-dependent conductance.

The anion selectivity of the ion pathway in case of the synthetic polypeptides implies that Cl^- permeates faster than K^+. Transmembrane ion movements are determined by the association and dissociation rates of the particular ions within the membrane pathway structure which, on the other hand, depend on the interactions of these ions with the space structure between the helices and/or with the helix dipoles. Evidence for the steric feasibility of such interactions was found by X-ray structure analysis of an α-helical undecapeptide which reveals dichloromethane molecules embedded between α-helical rods (Schmitt, Winter, Bosch & Jung, 1982). Furthermore, there are indications that α-helical regions are often involved in the binding of anions to proteins (Hol, 1985). Cation selectivity observed with alamethicin seems to be due to the additional hydrophilic amino acids at its C-terminal end.

Strongly Voltage-Dependent Conductance

Recently, a model was presented by Boheim et al. (1983) which explains the voltage-dependent con-

ductance induced by alamethicin in planar lipid membranes in terms of an electric field-induced flip-flop of single alamethicin molecules. Prior to voltage application alamethicin forms oligomeric aggregates of antiparallel-oriented helical rods. Then, due to the orientational forces of the membrane electric field, some molecules flip and a water-filled ion-translocating channel is formed by the circular arrangement of now parallel helices. We want to demonstrate that the data obtained with the synthetic polypeptides at large applied voltages easily fit into this dipole flip-flop gating model and thus yield further evidence for its actual realization in the presence of small helical molecules.

As shown in Fig. 1 the steady-state voltage-dependent conductivity λ_∞ induced by the polypeptides increases exponentially with the applied voltage. We write

$$\lambda_\infty \alpha \exp\{\alpha(\lambda_\infty) \cdot FV/RT\} \tag{1}$$

with $\alpha(\lambda_\infty) = 4.7$ for all the peptides. We will use the same notation as described by Boheim and Kolb (1978). Since we worked at significantly large values of the weakly voltage-dependent conductance in polypeptide modified bilayers, our experimental conditions can at best be compared to those of high λ_ϕ pretreatment (Boheim & Kolb, 1978).

The steady-state conductivity λ_∞ is determined not only by the applied voltage but also by the polypeptide concentration C_p of the membrane surrounding solution. This is shown in Fig. 3 on a double-logarithmic plot. The characteristic voltage V_c, which is needed to induce a bilayer conductivity of 100 μS/cm^2, is found to decrease when C_p is increased. We write

$$\lambda_\infty \propto (C_p)^{\delta(\lambda_\infty)} \cdot \exp\{\alpha(\lambda_\infty) \cdot FV/RT\}. \tag{2}$$

From the slope of the straight lines in Fig. 3 the power dependence of λ_∞ on the concentration C_p of each of the polypeptides studied is calculated to be $\delta(\lambda_\infty) = 8.3$. In contrast to the similar concentration dependences it was found that the reference concentration necessary to observe a given switch-on voltage V_c varies considerably with the different polypeptides. This reference concentration is higher the shorter the polypeptide chain. Since V_c is expected to depend on the actual polypeptide concentration in the membrane (Boheim & Kolb, 1978), we suppose that the differences in channel forming activity is merely an indication of the corresponding difference of peptide chains in the partition coefficients between aqueous and lipid phase. This is in good agreement with the fact that the polypeptides used are the more water soluble the shorter their chain length.

Voltage-jump current-relaxation curves revealed two exponentially increasing components of different amplitudes and time constants. We suggest that this is due to the simultaneous presence of two channel populations characterized by different mean lifetimes. This suggestion is supported by careful inspection of the single channel current fluctuation traces (Figs. 8 and 9). Similar results were obtained with alamethicin in frozen bilayers near the main phase transition temperature of the lipid used (Boheim et al., 1982). Figure 6 shows both time constants in dependence on the steady-state conductivity λ_∞ in a double-logarithmic plot. Implying again a power dependence we write

$$\tau_s \propto (\lambda_\infty)^{\beta(\tau_s)}. \tag{3}$$

$\beta(\tau_s)$ is approximately the same for all polypeptides, for both τ_s and τ_s^*. Its mean value is $\beta(\tau_s) = -0.58 + 0.01$. Since this value of β applies to both time constants, it may be allowed to combine Eqs. (2) and (3), in order to obtain a rough estimate for the power dependences of τ_s and τ_s^* on polypeptide concentration and applied voltage

$$\tau_s \propto (C_p)^{\delta(\tau_s)} \cdot \exp\{\alpha(\tau_s) \cdot FV/RT\}. \tag{4}$$

It is calculated $\delta(\tau_s) = -2.7$ and $\alpha(\tau_s) = -4.8$. τ_s and τ_s^* should be equal to the mean lifetime of the respective single channel types. On the basis of Fig. 6 and by use of the mean single channel conductances (Table 5) τ_s and τ_s^* may be calculated by extrapolation to λ_∞-values which correspond to an average of only 2–4 channels. We obtain $\tau_s = 2.5$ sec and $\tau_s^* = 200$ msec in case of P10, $\tau_s = 6.5$ sec and $\tau_s^* = 550$ msec for P20. We obtain a satisfactory agreement with the averaged open channel lifetimes of the two channel types, if the slow time constant τ_s is related to the long-lived channels and the faster time constant τ_s^* to the short-lived channels (Fig. 8).

A rough estimate of the concentration and voltage dependence of the channel formation rate may be obtained on the basis of several assumptions. First, current-relaxations in voltage-jump experiments are approximated by a sum of exponential functions, i.e., the delay period will be neglected. Second, the two channel expressions are considered to gate statistically independent of each other. According to Boheim and Kolb (1978) we write for each channel type

$$dN_p/dt = \mu - k_b N_p. \tag{5}$$

N_p is the number of activated channels in the bilayer

either of the long- or of the shorter-lived type, μ the channel formation rate (mol/(cm^2 · sec)) and k_b the pore decay rate (1/sec). It follows from Eq. (5) for the relaxation time constants

$$\tau_s = 1/k_b;\ \tau_s^* = 1/k_b^*.$$

Although the ratio of the two current amplitudes A_s/A_s^* varies with λ_∞ (Fig. 6*C*), i.e., long-lived channels occur mainly at low λ_∞ and increasing amounts of shorter-lived channels occur as λ_∞ increases, the associated time constants show similar variation with λ_∞. It should therefore be possible to neglect that change in amplitude distribution and assume the following steady state relation to be applicable to both channel types, at least with respect to their voltage and polypeptide concentration dependence

$$N_p = \mu \cdot \tau_s \tag{7}$$

thus

$$\lambda_\infty = \mu \cdot \tau_s \cdot \bar{\Lambda}. \tag{8}$$

$\bar{\Lambda}$ is the mean unit channel conductance and μ a somewhat averaged channel formation rate. Variables in Eq. (8) may be written as functions of V and C_p in the general form of Eqs. (2) and (4). Then the following relations hold for the two exponents $\alpha(\mu)$ and $\delta(\mu)$ (Boheim & Kolb, 1978)

$$\alpha(\mu) = \alpha(\lambda_\infty) - \alpha(\tau_s) - \alpha(\bar{\Lambda}) \tag{9}$$

$$\delta(\mu) = \delta(\lambda_\infty) - \delta(\tau_s) - \delta(\bar{\Lambda}). \tag{10}$$

Since $\bar{\Lambda}$ seems to be almost independent of both V and C_p, we will use as an upper limit $\alpha(\bar{\Lambda}) = \delta(\bar{\Lambda}) = 1$, which applies to the alamethicin channel (Boheim & Kolb, 1978). Hence from Eqs. (9) and (10) and from the above calculated values of $\alpha(\lambda_\infty)$, $\alpha(\tau_s)$, $\delta(\lambda_\infty)$ and $\delta(\tau_s)$ we obtain $\alpha(\mu) = 6.4$ and $\delta(\mu) = 12.1$.

The straightforward interpretation of these numbers would be the following: On the average a channel is formed out of a pre-existing aggregate of 12 molecules (indicated by the δ-exponent) and the actual channel formation process is initiated by the transfer of formally six elementary charges across the whole distance of membrane voltage drop (indicated by the α exponent). This feature is just a main prediction of the dipole flip-flop gating model (Boheim et al., 1983), since pre-existing dodecamers should consist of six dimer pairs of antiparallel-arranged helix dipoles. The application of a sufficiently high electric field will force all helices to assemble in parallel array, i.e., six molecules "flip." The net transfer of six elementary charges is equivalent to the transfer of 6/2 positive charges into one and 6/2 negative charges into the opposite direction. The latter gating charge movement applies to α-helices (Hol, 1985).

It is not surprising that all polypeptides (P5 to P20) display the same potential dependence despite their large difference in chain length. Provided that the full voltage drop occurs along an inserted α-helix, the electric field strength increases just with the same factor by which the dipole moment is decreased, thus leaving the electrostatic energy situation unchanged. The energy, which is required to convert an aggregate of four helices (of 20 amino acids) from antiparallel to parallel arrangement in a medium of dielectric constant 2, is estimated to be 37 kcal/mol (Hol et al., 1981; Hol, 1985). Roughly one half of that value is expected, if finally the parallel helices lie in a medium of large dielectric constant. This situation applies to the water-filled channel. An energy of 8–9 kcal/mol per α-helix is available at an applied voltage of 250–300 mV in order to reverse its transmembrane orientation. Near that voltage range at room temperature helices may flip from antiparallel-to-parallel orientation in quantitative agreement with the switch-on voltage measurements in our work.

Let us consider the concentration and voltage dependence of the steady-state conductance λ_∞, which is characterized by the exponential factors $\alpha(\lambda_\infty)$ and $\delta(\lambda_\infty)$. The values are significantly smaller than those of the channel formation rate. This observation may reflect an actual reduction in channel size, i.e., the channel is formed as dodecameric aggregate and thereafter decreases to octameric size by sequential dissociation of monomers. Instability of large size aggregates may be caused by unfavorable electrostatic interactions between the parallel helices. A similar observation of channel size reduction has been reported for alamethicin (Boheim & Kolb, 1978). In addition, channel size reduction explains two experimental phenomena: saturation of the conductance/voltage curve at high values of λ_∞ (Fig. 1*B*) and inactivation of the current-relaxation curves under conditions of large λ_∞ (Fig. 7*B*).

Delay of channel activation (*S*-shaped time course, Fig. 7*A*) as well as inactivation behavior (Fig. 7*B*) are intrinsic properties of sequential aggregation mechanisms (Mueller, 1976). Apart from that obvious similarity, relaxation experiments revealed a characteristic difference in the answers to voltage-sign reversal of P5 to P20 on one side and alamethicin on the other. The polypeptides constitute rods of linear structure, and the vector of the dipole moment lies parallel to the helix axis. After orientation in an electric field this dipole-moment vector and the electric field vector are parallel, exhibiting no vertical force component. In characteristic contrast

the alamethicin helix is bent at the Pro(14) residue. Consequently, the main helix axis and the vector of the resulting dipole moment deviate. It seems to be quite unlikely that the externally applied electric field and the resulting dipole moment have parallel orientation. Besides a parallel component, therefore, a second vector component of the helix dipole moment may exist which lies within the membrane plane. Its interaction with the electric field vector yields a torque which attacks each alamethicin molecule. Figure 4*A* shows that alamethicin channels are immediately destroyed upon abrupt sign reversal of the membrane voltage. As pointed out, this torque may initiate molecule movement out of the now unstable orientation antiparallel to the applied electric field. Subsequent flipping of the entire helical molecule destroys the existing channel but then creates a new one with opposite helix orientation within the membrane. In strict contrast, the polypeptide rods do not give rise to such a torque. These helices are not forced to flip immediately after voltage sign reversal but remain in the metastable position (Fig. 4*B*). However, if for a short time the orientating electric field is turned off (zero applied voltage), thermal disordering causes the polypeptides to leave that position normal to the membrane plane and a small horizontal component of the dipole moment establishes. The torque resulting from the interaction of this vector component with the vertical, newly applied electric field leads to immediate closure of all channels previously formed (Fig. 4*C*). Comparable to the situation with alamethicin new channels start to form from the bare membrane level.

The relaxation time constants are related to the rate constants of channel decay (Eq. (6)). In Table 4 a series of relaxation times at comparable steady-state conductance and applied voltage are listed for P5 to P20 and alamethicin. With reference to the activation energy for channel decay of P10 the corresponding barriers of P15, P20 and alamethicin are higher by 0.6, 0.9 and 2.75 kcal/mol, respectively. P5 behaves similarly to P10, indicating dimer formation (*see below*).

Unit Channel Conductance

The dipole flip-flop gating model predicts that the length of the ion channel should correspond to the length of the α-helix. In order to test this hypothesis we want to compare the values of single channel conductances of the various polypeptides (Table 5). It is assumed that under the conditions of Fig. 8 the different polypeptide channels are formed by the same average number of monomers assembled in circular array, according to the barrel-stave model (Finkelstein & Holz, 1973; Boheim et al., 1983). Then the unit conductance of a particular channel should be inversely related to its length by

$$\bar{\Lambda} = (\pi r^2/1) \cdot \sigma \tag{11}$$

where σ is the conductivity of the solution which fills the channel and r and l are radius and length of the channel, respectively. The assumption made above implies the same radius for all helical channels, i.e., the product $\bar{\Lambda} \cdot l$ should remain constant independent of the polypeptide chain length. As shown in Table 5 P20, P15 and P10 follow Eq. (11) to a good approximation, while P5 fails to do so. However, it fits into the scheme if one considers a channel length twice that of the single chain. This means that the staves of the P5 barrel seem to be built up of two head-to-tail linked helices. In fact, crystal structure analysis of 15 different Aib-containing penta- to undecapeptides (including P5a, P9 and P11) revealed extended rods of head-to-tail linked monomers in antiparallel orientation (Bosch et al., 1984). Irrespective of α- or 3_{10}-helical structure, molecules interact by van der Waals forces of their lipophilic side chains and by one or two hydrogen bridges at the head-to-tail contact. Furthermore, Hol, van Duijnen and Berendsen (1978) have shown that the electric field measured along an α-helix axis is quite large in proximity of its termini. In low dielectric medium the potential at a distance of 5 Å from the end of a five-residue α-helix is roughly 500 mV and increases to a maximum value of 1.5 V upon reducing this distance (Hol et al., 1978). Thus an energy gain of about 17.5 kcal/mol (30 *RT*) is calculated for head-to-tail dimerization of two pentapeptides. We therefore suppose that all pentapeptides embedded into the bilayer adopt the head-to-tail dimerized state, i.e., that of a quasi-decapeptide. This explains the similarities in channel forming properties of P5 and P10. It is worth mentioning that head-to-tail aggregation was also observed with alamethicin and trichotoxin in octanol (Schwarz & Savko, 1982; Schwarz et al., 1983).

Chain lengths of the various helices were estimated in Table 5 using the following distances per amino acid (Bosch, 1984): 1.5 Å (α-helix) and 2.0 Å (3_{10}-helix). In case of P5 two possible chain lengths are given, because it cannot be excluded that the 3_{10}-helical pentapeptide dimer might adopt the α-helical conformation of the decapeptide under the influence of the high membrane electric field. The thickness of the hydrophobic core of a comparable solvent-free lipid bilayer membrane was estimated to be about 25 Å (Boheim, Hanke & Eibl, 1980). Therefore, helix lengths of 22.5 Å (P15) or 30 Å (P20) may bridge the bilayer without significant problems. However, a channel of 15 Å length (P10

and P5-dimer) can only be stabilized by local distortions of the bilayer lipid. Such a stabilization has to occur without breakdown of the bilayer structure. Even the lateral separation into large dodecamer aggregates of antiparallel or parallel helix orientation needs to be tolerated. This surprising fact may be explained by strong hydrophobic interactions between the unpolar amino acid side chains and the lipophilic hydrocarbon chains.

The single channel data in Table 5 enable us to give a rough estimate of the diameter of the polypeptide channels. Figure 10*D* shows that also the alamethicin channel becomes stabilized at a preferred conductance level at high applied voltages. Using the level numbers of Hanke and Boheim (1980), which comprise also the lowest conductance state, most probably levels 7 ± 1 are adopted. This would correspond to a channel radius of 1.9 ± 0.2 nm, if one assumes that the specific conductance of a large aqueous ion channel equals the conductivity of the bulk solution (Hanke & Boheim, 1980). Structural model considerations of helix packing in circular arrangement supports the concept that most likely the 1st conducting state is formed by four helices. Then the 7th conductance level would be established by 10 helices, in excellent agreement with the polypeptide concentration dependences observed. The inner diameter of a decamer channel was estimated by use of the crystallographic radii of the polypeptide helices to be 2.1 nm for α-helical and 1.9 nm for 3_{10}-helical rods (Bosch, 1984). This confirms our assumption that conductances of large size channels are determined by bulk solution conductivity. In addition, it explains the poor ionic selectivity of the polypeptide channels. We want to emphasize the fact that the purely hydrophobic polypeptides P5, P5a, P9, P10, P11, P15 and P20 as well as alamethicin and its natural analogs form transmembrane ion channels in a similar way. Independent of the helix type, i.e., α-helix, 3_{10}-helix or mixed $\alpha/3_{10}$-helix, the strongly voltage-dependent channel properties are observed in each case originating from their respective helix dipole moment.

The flip-flop barrel-stave model implies that each channel can undergo transitions between different conductance levels, which correspond to different numbers of staves comprising the barrel. The occurrence of fast transitions between neighboring levels also in case of the synthetic polypeptides is strongly evidenced by the increased noise amplitude of the open channel current trace (Fig. 8). By cooling the membrane system to 5°C discrete fluctuations between different conductance levels of the same channel were resolved, indeed (Fig. 10). Nevertheless, a single given channel seems to be stabilized and to live most of the time in one well-defined conductance state, whereby the broad distribution of a multitude of channel conductances may reflect a corresponding distribution of the aggregate size, i.e., of the number of monomers involved in channel formation.

Channel Formation by Natural and Other Related Polypeptides

Experiments with alamethicin clearly show that this antibiotic acts very similarly to P5 to P20 at the high applied voltages, whereas a slightly different behavior is observed at voltages $\lesssim 150$ mV. The *I/V* curves (Figs. 2 and 3) yield $\alpha(\lambda_\infty) = 6$ and $\delta(\lambda_\infty) = 10.5$. Considering the current-relaxation experiments (Fig. 6) we obtain $\alpha(\tau_s) = -1.2$ and $\delta(\tau_s) = -2.1$. Using again Eqs. (9) and (10) the exponential parameters of the pore formation rate can be estimated at $\alpha(\mu) = 6.2$ and $\delta(\mu) = 11.6$, which are almost the same as obtained with the synthetic polypeptides. Thus channels seem to preferentially open out of dodecameric aggregates with a transmembrane transfer of six formal elementary charges. Significantly different from those of P5 to P20 are the larger lifetimes of alamethicin channels. This may be due to the bigger hydrophilic C-terminus of alamethicin which increases the activation energy for transbilayer reorientations. A comparable stabilizing effect was observed with the C-terminally dansylated trichotoxin derivative (Hanke et al., 1983).

A few chemically modified analogs of alamethicin were studied recently (Vodyanoy, Hall, Balasubramanian & Marshall, 1982; Jung et al., 1983*a*; Hall, Vodyanoy, Balasubramanian & Marshall, 1984), including Boc-2-20-alamethicin, BG-alamethicin with positively charged free amino terminus and alamethicin-17, which lacks the C-terminal sequence Glu-Gln-Pheol. Interestingly, all these analogs induce strongly voltage-dependent conductances in lipid bilayers similar to alamethicin. Hall et al. (1984) proposed a mixed α-helix (N-terminal sequence)/β-barrel (C-terminal sequence) structure for the channel forming molecules. The fact, however, that the voltage-dependent behavior of alamethicin-17 is the same as that of natural alamethicin, although it lacks the assumed β-barrel stabilizing hydrophilic C-terminus, gives strong evidence for an exclusively helical structure of the antibiotic. The helical structure of P9, the C-terminal nonapeptide of alamethicin, was confirmed by X-ray analysis of P9 crystals (Bosch et al., 1985*b*). Jung et al. (1983*a*) showed in addition that Boc-2-20-alamethicin behaves very similarly to P5 to P20 with respect to *I/V*-characteristics as well as to the

particularly large single channel conductance values at high membrane voltages. This similarity seems to result from the same N-terminal Boc-group (G. Boheim & S. Gelfert-Peukert, *to be published*).

Series of experiments with synthetic helical polypeptides were carried out and reported by Mathew and Balaram (1983*a*). Unfortunately, these measurements were taken without using electrochemical methods or planar bilayer techniques. Since most of these synthetic short-chained polypeptides induce the weakly voltage-dependent conductance in the absence of an applied membrane voltage as described above, vesicle flux measurements do not give information on voltage-dependent effects. This method cannot even discriminate between ion transport by carriers or through channels. The "core piece ejection" model proposed by Mathew and Balaram (1983*b*) seems not to be applicable to P5 to P20 or alamethicin. Dipoles usually move along a gradient towards the higher electric field strength, i.e., into the lipid phase and not into the low-field aqueous phase.

The results obtained in presence of the natural polypeptide antiamoebin (Figs. 2 and 3) suggest that a channel forming mechanism similar to that discussed above also applies in this case. However, some differences exist. The *I/V*-curve in Fig. 2*B* indicates very slow reaction processes during channel formation, since current still increases although voltage already decreases. Consistent with this behavior is the strongly expressed delay and *S*-shaped time course in voltage-jump current-relaxation experiments (W. Hanke, *personal communication*). At high applied voltages discrete conductance steps were observed, too, but of smaller 1–2 nS amplitude (*data not shown*). Circular dichroism studies show no significant α-helix formation by antiamoebin in organic solvents (Brückner, Graf & Bokel, 1984). The strong voltage-dependence of channel formation, however, points to a rod-like shape within the lipid bilayer phase of presumably helical structure.

It is interesting to note that the channel formation properties of the polypeptides and especially of antiamoebin resemble those of monazomycin (Muller & Finkelstein, 1972). The polyene structure of the antibiotic monazomycin has been solved by Nakayama, Furihata, Seto and Otake (1981) and found to contain a large number of hydroxyl groups and one amino group providing a single positive charge. The rod-like shape of the molecule is compatible with the barrel-stave model proposed for the related channel former amphotericin B by Finkelstein and Holz (1973). The channel lumen is most probably lined by the polar hydroxyl groups, and the positive charge imposes the voltage-dependent effects in channel gating. Although the behavior of their respective ion channels is apparently the same, there are no similarities in the molecular structures of monazomycin and the polypeptides P5 to P20. Monazomycin is amphiphil all along this rod-shaped molecule. If no voltage is applied, it would swim on the membrane surface with its hydrophobic side oriented towards the bilayer lipid phase and its hydrophilic side in contact with the aqueous solution. Upon voltage application the positive charge is transferred across the bilayer. Simultaneously the molecule bridges the membrane and by rod aggregation in parallel array the channels are formed. The strong delay and final inactivation of the monazomycin-induced current after voltage jumps was interpreted in terms of autocatalytic channel formation (Muller & Andersen, 1982) and net transfer of monazomycin across the bilayer (Heyer, Muller & Finkelstein, 1976). The two possible positions of monazomycin, i.e., perpendicular to the membrane plane within the bilayer core and parallel to it at the membrane interface, seem to determine its behavior.

The situation is different with the completely hydrophobic polypeptides P5 to P20. At zero applied voltage the energetically preferred state in equilibrium would be that of aggregated antiparallel dipoles within the bilayer core oriented perpendicular to the membrane plane. Channel formation presumably occurs by dipole flip-flop, and the channel lumen seems to be lined by structured water (Edmonds, 1980). Our data support the idea that alamethicin, which has its hydrophilic molecule part concentrated at the C-terminal end, behaves similarly to the synthetic helical polypeptides. In contrast antiamoebin, which possesses a few hydrophilic amino acids (Hyp, Gln) within the amino acid chain (Table 1), may act like monazomycin. Delay in activation and current inactivation may as well be explained by autocatalytic insertion and molecule transfer during the channel-formation process.

The steady-state conductance λ_∞ induced by monazomycin in planar bilayers follows an exponential law of the type given in Eq. (2) with $\alpha(\lambda_\infty) = 5$ and $\delta(\lambda_\infty) = 5$ (Muller & Finkelstein, 1972). Current relaxation curves reveal that the time constant of the exponential rising phase decreases when λ_∞ is increased (Muller & Finkelstein, 1972; Heyer et al., 1976). Single channel events mostly appear as on/off transitions with broad distributions of conductance values. Sometimes transitions between various neighboring conductance levels of the same open channel were resolved (Andersen & Muller, 1982). The mean conductance value of the monazomycin channel, $\bar{\Omega} = 5$ pS in 0.1 M NaCl, is orders of magnitude lower than that of the polypeptides, but

comparable to the lowest conductance state of the alamethicin channel (Hanke & Boheim, 1980). Channel lumen diameters of about 8 Å were estimated by tracer flux measurements for the structurally related polyene antibiotics amphotericin B and nystatin (Finkelstein & Holz, 1973). If this value is applied also to the monazomycin channel, its mean conductance appears to be surprisingly low for a "hydrophilic" channel as compared to the "hydrophobic" polypeptide helix channels.

A further interesting finding was reported on the polyenes nystatin and amphotericin B. Both antibiotics form two types of channels which differ in their mean conductance and ion selectivity (Marty & Finkelstein, 1975; Kleinberg & Finkelstein, 1984). The first channel type is established by monomers and the second type by tail-to-tail linked dimers. The barrel-stave array seems to be adopted in both cases. Since no fixed charge exists at the two polyenes, tail-to-tail dimerization should be possible. This is different for the polypeptides P5 and P5a, which have to undergo head-to-tail dimerization due to dipole interactions. As in the case of monazomycin the unit channel conductances are extremely small. In 2 M KCl 5 pS for the one-sided and 1 pS for the two-sided nystatin channel are found (Kleinberg & Finkelstein, 1984), which is three to four orders of magnitude smaller than the mean conductances of the P10 and P5 channels.

Different from the behavior of the synthetic polypeptides discussed above, poly(AAG) exhibits only a low voltage dependence in the polypeptide-induced current increase. We did not succeed in observing single channel current fluctuations, presumably because of the simultaneous presence of peptide chains of different lengths. However, the comparably low voltage dependence of membrane current increase agrees with the data presented by Urry et al. (1978) and may exclude α-helical conformation of poly(AAG) within the bilayer (Spach, Trudelle & Heitz, 1983).

We thank Dr. A. Brack and Dr. G. Spach for the sample of synthetic poly(AAG) and Dr. W. Hanke for helpful discussions. This work was financially supported by the Deutsche Forschungsgemeinschaft (SFB 114).

References

Andersen, O.S., Muller, R.U. 1982. Monazomycin-induced single channels: I. Characterization of the elementary conductance events. *J. Gen. Physiol.* **80:**403–426

Boheim, G. 1974. Statistical analysis of alamethicin channels in black lipid membranes. *J. Membrane Biol.* **19:**277–303

Boheim, G., Hanke, W., Eibl, H. 1980. Lipid phase transition in planar bilayer membrane and its effect on carrier- and pore-mediated ion transport. *Proc. Natl. Acad. Sci. USA* **77:**3403–3407

Boheim, G., Hanke, W., Jung, G. 1983. Alamethicin pore formation: Voltage-dependent flip-flop of α-helix dipoles. *Biophys. Struct. Mechan.* **9:**181–191

Boheim, G., Hanke, W., Überschär, S., Eibl, H. 1982. Alamethicin pore formation in planar bilayers above and below lipid phase transition temperature. *In:* Transport in Biomembranes: Model Systems and Reconstitution. R. Antolini, et al., editors. pp. 135–143. Raven, New York

Boheim, G., Janko, K., Leibfritz, D., Ooka, T., König, W.A., Jung, G. 1976. Structural and membrane modifying properties of suzukacillin, a peptide antibiotic related to alamethicin. Part B: Pore formation in black lipid films. *Biochim. Biophys. Acta* **433:**182–199

Boheim, G., Kolb, H.A. 1978. Analysis of the multi-pore system of alamethicin in a lipid membrane: I. Voltage-jump current-relaxation experiments. *J. Membrane Biol.* **38:**99–150

Bosch, R. 1984. Röntgenstrukturanalysen und vergleichende Studien von Alamethicin-Segmenten mit β-Turns, $3^{\downarrow}_{10}$- und $3^{\prime}_{10}$-, sowie α-Helices. Ph.D. Thesis. University of Tübingen, Tübingen

Bosch, R., Jung, G., Schmitt, H., Sheldrick, G.M., Winter, W. 1984. Peptide structures of the alamethicin sequence: The C-terminal $\alpha/3_{10}$-helical nonapeptide and two pentapeptides with opposite 3_{10}-helicity. *Angew. Chem. Int. Ed. Engl.* **23:**450–453

Bosch, R., Jung, G., Schmitt, H., Winter, W. 1985*a*. Crystal structure of the α-helical undecapeptide Boc-L-Ala-Aib-Ala-Aib-Ala-Glu(OBzl)-Ala-Aib-Ala-Aib-Ala-OMe. *Biopolymers* **24:**961–978

Bosch, R., Jung, G., Schmitt, H., Winter, W. 1985*b*. Crystal structure of Boc-Leu-Aib-Pro-Val-Aib-Aib-Glu(OBzl)-Gln-Phl · H_2O, the C-terminal nonapeptide of the voltage-dependent ionophore alamethicin. *Biopolymers* **24:**979–999

Bosch, R., Jung, G., Winter, W. 1983. Structure of the 3_{10}-helical pentapeptide Boc-Aib-L-Ala-Aib-L-Ala-Aib-OMe · 2 H_2O. *Acta Crystallogr. Sect. C* **39:**776–778

Brückner, H., Graf, H., Bokel, M. 1984. Paracelsin: Characterization by NMR spectroscopy and circular dichroism, and hemolytic properties of a peptaibol antibiotic from the cellulolytically active mold *Trichoderma reesei*. Part B. *Experientia* **40:**1189–1197

Brückner, H., Jung, G. 1982. Synthesis of L-Pro-Leu-Aib-Aib-Gln-Valol and proof of identity with the isolated C-terminal fragment of trichotoxin A40. *Liebigs Ann. Chem.* **1982:**1677–1699

Brückner, H., König, W.A., Aydin, M., Jung, G. 1985. Trichotoxin A40. Purification by counter current distribution and sequencing of isolated fragments. *Biochim. Biophys. Acta* **827:**51–62

Brückner, H., Nicholson, G.J., Jung, G., Kruse, K., König, W.A. 1980. Gas chromatographic determination of the configuration of isovaline in antiamoebin, samarosporin (emerimicin IV), stilbellin, suzukacillins and trichotoxins. *Chromatographia* **13:**209–214

Brückner, H., Przybylski, M. 1984. Isolation and structural characterization of polypeptide antibiotics of the peptaibol class by HPLC with FD and FAB mass spectrometry. *J. Chromat.* **296:**263–275

Butters, T., Hütter, P., Jung, G., Pauls, N., Schmitt, H., Sheldrick, G.M., Winter, W. 1981. On the structure of the helical N-terminus in alamethicin–α-helix or 3_{10}-helix? *Angew. Chem. Int. Ed. Engl.* **20:**889–890

Davis, P.J., Fleming, B.D., Coolbear, K.P., Keough, K.M.W. 1981. Gel to liquid-crystalline transition temperatures of water dispersions of two pairs of positional isomers of unsaturated mixed-acid phosphatidylcholines. *Biochemistry* **20:**3633–3636

Edmonds, D.T. 1980. Membrane ion channels and ionic hydration energies. *Proc. R. Soc. London B* **211:**51–62

Eisenberg, M., Hall, J.E., Mead, C.A. 1973. The nature of the voltage-dependent conductance induced by alamethicin in black lipid membranes. *J. Membrane Biol.* **14:**143–176

Finkelstein, A., Holz, R. 1973. Aqueous pores created in thin lipid membranes by the polyene antibiotics nystatin and amphotericin B. *In:* Membranes. Vol. 2. Lipid Bilayers and Antibiotics. G. Eisenman, editor. pp. 377–408. M. Dekker, New York

Fox, R.O., Richards, F.M. 1982. A voltage-gated ion channel model inferred from crystal structure of alamethicin at 1.5 Å resolution. *Nature (London)* **300:**325–330

Gordon, L.G.M., Haydon, D.A. 1972. The unit conductance channel of alamethicin. *Biochim. Biophys. Acta* **255:**1014–1018

Hall, J.E., Vodyanoy, I., Balasubramanian, T.M., Marshall, G.R. 1984. Alamethicin—A rich model for channel behavior. *Biophys. J.* **45:**233–247

Hanke, W., Boheim, G. 1980. The lowest conductance state of the alamethicin pore. *Biochim. Biophys. Acta* **596:**456–462

Hanke, W., Methfessel, C., Wilmsen, H.-U., Katz, E., Jung, G., Boheim, G. 1983. Melittin and a chemically modified trichotoxin form alamethicin-type multi-state pores. *Biochim. Biophys. Acta* **727:**108–114

Heyer, E.J., Muller, R.U., Finkelstein, A. 1976. Inactivation of monazomycin-induced voltage-dependent conductance in thin lipid membranes: II. Inactivation produced by monazomycin transport through the membrane. *J. Gen. Physiol.* **67:**731–748

Hol, W.G.J. 1985. The role of the α-helix dipole in protein function and structure. *Prog. Biophys. Molec. Biol.* **45:**149–195

Hol, W.G.J., Duijnen, P.T. van, Berendsen, H.J.C. 1978. The α-helix dipole and the properties of proteins. *Nature (London)* **273:**443–446

Hol, W.G.J., Halie, L.M., Sander, C. 1981. Dipoles of the α-helix and β-sheet: Their role in protein folding. *Nature (London)* 294:532–536

Jung, G., Becker, G., Schmitt, H., Voges, K.-P., Boheim, G., Griesbach, S. 1983*a*. Voltage-gated membrane pores are formed by a flip-flop of α-helical polypeptides. *In:* Peptides, Structure and Function. V.J. Hruby, and D.H. Rich, editors. pp. 491–494. Pierce Chemical Co., Rockford, Ill.

Jung, G., Bosch, R., Katz, E., Schmitt, H., Voges, K.-P., Winter, W. 1983*b*. Stabilizing effects of 2-methylalanine residues on β-turns and α-helices. *Biopolymers* **22:**241–246

Jung, G., Dubischar, N., Leibfritz, D. 1975. Solvent and temperature induced conformational changes of alamethicin, a ^{13}C NMR and circular dichroism study. *Eur. J. Biochem.* **54:**395–409

Jung, G., Katz, E., Schmitt, H., Voges, K.-P., Menestrina, G., Boheim, G. 1983*c*. Conformational requirements for the potential dependent pore formation of the peptide antibiotics alamethicin, suzukacillin and trichotoxin. *In:* Physical Chemistry of Transmembrane Ion Motions. G. Spach, editor. pp. 349–357. Elsevier, Amsterdam

Katz, E., Aydin, M., Lucht, N., König, W.A., Ooka, T., Jung, G. 1985. Sequence and conformation of suzukacillin A. *Liebigs Ann. Chem.* **1985:**1041–1062

Kleinberg, M.E., Finkelstein, A. 1984. Single-length and double-length channels formed by nystatin in lipid bilayer membranes. *J. Membrane Biol.* **80:**257–269

Marty, A., Finkelstein, A. 1975. Pores formed in lipid bilayer membranes by nystatin. Differences in its one-sided and two-sided action. *J. Gen. Physiol.* **65:**515–526

Mathew, M.K., Balaram, P. 1983*a*. Alamethicin and related membrane channel forming polypeptides. *Mol. Cell. Biochem.* **50:**47–65

Mathew, M.K., Balaram, P. 1983*b*. A dipole helix model for alamethicin and related transmembrane channels. *FEBS Lett.* **157:**1–5

McIntosh, T.J., Ting-Beall, H.P., Zampighi, G. 1982. Alamethicin induced changes in lipid bilayer morphology. *Biochim. Biophys. Acta* **685:**51–60

Montal, M., Mueller P. 1972. Formation of bimolecular membranes from lipid monolayers and a study of their electrical properties. *Proc. Natl. Acad. Sci. USA* **69:**3561–3566

Mueller, P. 1976. Molecular aspects of electrical excitation in lipid bilayers and cell membranes. *Horizons Biochem. Biophys.* **2:**230–284

Mueller, P., Rudin, D.O. 1968. Action potentials induced in bimolecular lipid membranes. *Nature (London)* **217:**713–719

Muller, R.U., Andersen, O.S. 1982. Monazomycin-induced single channels. II. Origin of the voltage dependence of the macroscopic conductance. *J. Gen. Physiol.* **80:**427–449

Muller, R.U., Finkelstein, A. 1972. Voltage-dependent conductance induced in thin lipid membranes by monazomycin. *J. Gen. Physiol.* **60:**263–284

Nakayama, H., Furihata, K., Seto, H., Otake, N. 1981. Structure of monazomycin, a new ionophorous antibiotic. *Tetrahedron Lett.* **22:**5217–5220

Rinehart, K.L., Cook, J.C., Meng, H., Olson, K.L., Pandey, R.C. 1977. Mass spectrometric determination of molecular formulas for membrane-modifying antibiotics. *Nature (London)* **269:**832–833

Rizzo, V., Schwarz, G., Voges, K.-P., Jung, G. 1985. Molecular shape and dipole moment of alamethicin-like synthetic peptides. *Eur. Biophys. J.* **12:**67–73

Robinson, R.A., Stokes, R.H. 1959. Electrolyte Solutions. Butterworth, London

Roy, G. 1975. Properties of the conductance induced in lecithin bilayer membranes by alamethicin. *J. Membrane Biol.* **24:**71–85

Schmitt, H., Jung, G. 1985*a*. Total synthesis of the α-helical eicosapeptide antibiotic alamethicin. *Liebigs Ann. Chem.* **1985:**321–344

Schmitt, H., Jung, G. 1985*b*. ^{13}C NMR spectroscopic control of the synthesis of Alamethicin F30 and its segments. *Liebigs Ann. Chem.* **1985:**345–364

Schmitt, H., Winter, W., Bosch, R., Jung, G. 1982. The α-helical conformation of the undecapeptide Boc-L-Ala-(Aib-Ala)$_2$-Glu(OBzl)-Ala-(Aib-Ala)$_2$-OMe: Synthesis, X-ray crystal structure, and conformation in solution. *Liebigs Ann. Chem.* **1982:**1304–1321

Schwarz, G., Savko, P. 1982. Structural and dipolar properties of the voltage dependent pore former alamethicin in octanol/dioxane. *Biophys. J.* **39:**211–219

Schwarz, G., Savko, P., Jung, G. 1983. Solvent dependent structural features of the membrane active peptide trichotoxin A40 as reflected in its dielectric dispersion. *Biochim. Biophys. Acta* **718:**419–428

Spach, G., Trudelle, Y., Heitz, F. 1983. Peptides as channel-

making ionophores: Conformational aspects. *Biopolymers* **22:**403–407

Urry, D.W., Bradley, R.J., Ohnishi, T. 1978. Characterization of a synthetic, voltage-dependent, cation-selective transmembrane channel. *Nature (London)* **274:**382–383

Vodyanoy, I., Hall, J.E., Balasubramanian, T.M., Marshall, G.R. 1982. Two purified fractions of alamethicin have different conductance properties. *Biochim. Biophys. Acta* **684:**53–58

Voges, K.-P. 1985. Zur Eintauchtiefe helikaler Tryptophanyl-Heneikosapeptide in Membranen: Synthese, NMR, CD und Fluoreszenz. Thesis, University of Tübingen, Tübingen

Yantorno, R.E., Takashima, S., Mueller, P. 1982. Dipole moment of alamethicin as related to voltage-dependent conductance in lipid bilayers. *Biophys. J.* **38:**105–110

Received 4 November 1985; revised 6 May 1986